

Source: Document 4-5-6-7/584 (Annex 11,
Attachment 7) (edited)

**Annex 15 to
Document 4-5-6-7/715-E
19 August 2014
English only**

Annex 15 to Joint Task Group 4-5-6-7 Chairman's Report

DRAFT NEW REPORT ITU-R SA.[EESS-IMT 2 025-2 290 MHz]

Sharing between space-to-space links in space research, space operation and Earth exploration-satellite services and IMT systems in the frequency bands 2 025-2 110 MHz and 2 200-2 290 MHz

1 Introduction

WRC-15 agenda item 1.1 called for conducting sharing and compatibility studies with services already having allocations in candidate frequency bands for potential accommodation of International Mobile Telecommunication (IMT) systems. The frequency bands 2 025-2 110 MHz and 2 200-2 290 MHz have been identified as suitable frequency ranges for accommodation of IMT systems.

Incumbent primary services in the frequency band 2 200-2 290 MHz include space operation (space-to-Earth and space-space), Earth exploration-satellite (space-to-Earth and space-space), fixed, mobile including aeronautical telemetry, and space research (space-to-Earth and space-to-space). Incumbent primary services in the frequency band 2 025-2 110 MHz include space operation (Earth-to-space and space-space), Earth exploration-satellite (Earth-to-space and space-space), fixed, mobile, and space research (Earth-to-space and space-to-space).

The allocation to the mobile service in this band is under the limitation of RR No. **5.391**:

5.391 *In making assignments to the mobile service in the bands 2 025-2 110 MHz and 2 200-2 290 MHz, administrations shall not introduce high-density mobile systems, as described in Recommendation ITU-R SA.1154, and shall take that Recommendation into account for the introduction of any other type of mobile system. (WRC-97)*

This report considers the feasibility of long term evolution (LTE) type of IMT systems sharing the frequency bands 2 025-2 110 MHz and 2 200-2 290 MHz with incumbent primary services of the space research, Earth exploration-satellite and space operation services in the space-to-space direction. Sections 4.1.1 and 4.2.1 examine the sharing potential of commercial broadband systems with forward link transmissions from NASA geostationary tracking and data relay satellite system (TDRSS) satellites in the frequency band 2 025-2 110 MHz to some typical satellite users, which are in low earth orbit (LEO). These are typical of the many forward link systems of various data relay satellite (DRS) satellites and user spacecraft. The protection of DRS forward links is critical to several administrations Earth science and space exploration programs as well as cooperative programs involving space agencies from around the world and authorized non-governmental user satellite operators.

Sections 4.2.1 and 4.2.2 examine the sharing potential of commercial broadband systems with return link transmissions of geostationary tracking and data relay satellite system satellites in the frequency band 2 200-2 290 MHz from the International Space Station (ISS), which is in low Earth orbit. These are typical of the many return link systems of various data relay satellites and user spacecraft. The protection of DRS return links is critical to several administrations' Earth science and space exploration programs as well as cooperative programs involving space agencies from around the world and authorized non-governmental user satellite operators.

This report does not include analyses of LTE sharing with other incumbent services and systems in the 2 025-2 110 MHz and 2 200-2 290 MHz frequency bands, such as proximity links with the International Space Station, satellite space-to-Earth links, and aeronautical mobile telemetry or other low-density mobile systems. As a result of the findings of these sharing analyses, namely that sharing between commercial broadband systems and data relay satellite systems precludes the accommodation of LTE systems, it is considered unnecessary to study other incumbent services in the frequency bands 2 025-2 110 MHz and 2 200-2 290 MHz.

An overview of the technical parameters used for this study is presented in section 3. Detailed technical characteristics, including calculation steps and analysis procedures, are presented in Appendices A-E.

The technical parameters for LTE systems in section 3 and the Appendices of this study are consistent with the agreed upon characteristics provided in Report ITU-R M.2292.

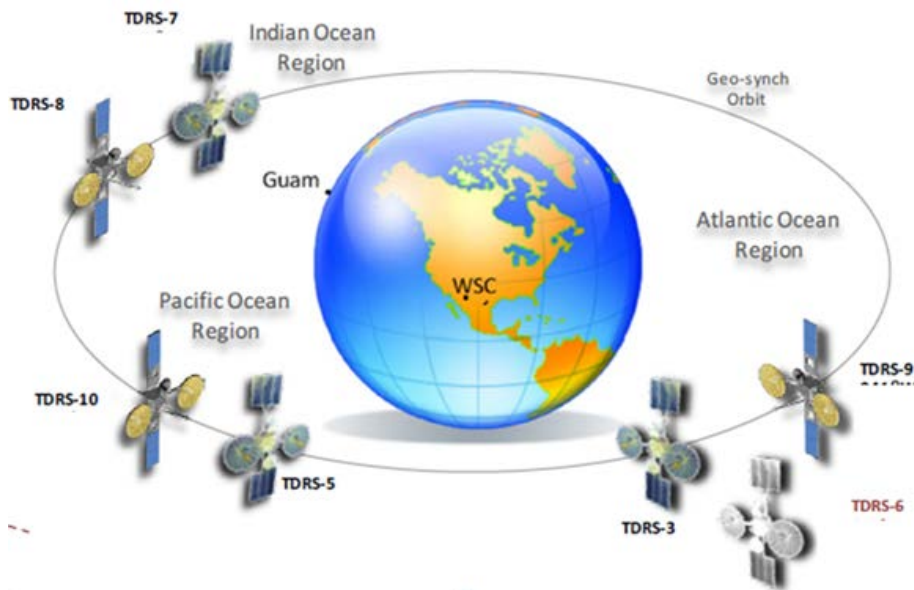
2 Background

This section provides background on the systems and parameters that were used for the sharing analysis between commercial broadband systems and DRS return links in the frequency bands 2 025-2 110 MHz and 2 200-2 290 MHz.

2.1 TDRSS

The tracking data and relay satellite system comprises six on-orbit tracking and data relay satellites located in geosynchronous orbit. Multiple additional TDRSSs are available as backups for operational support at any given time. The TDRSS is a relay system which provides continuous, highly reliable, worldwide tracking and data relay services between low earth orbiting spacecraft and earth stations that are interconnected with command centres and data processing facilities. Figure 1 presents an overview of the TDRSS constellation operating at locations around the world. Several other DRS satellites not shown in Figure 1 are operated by other administrations.

FIGURE 1
Overview of TDRSS constellation

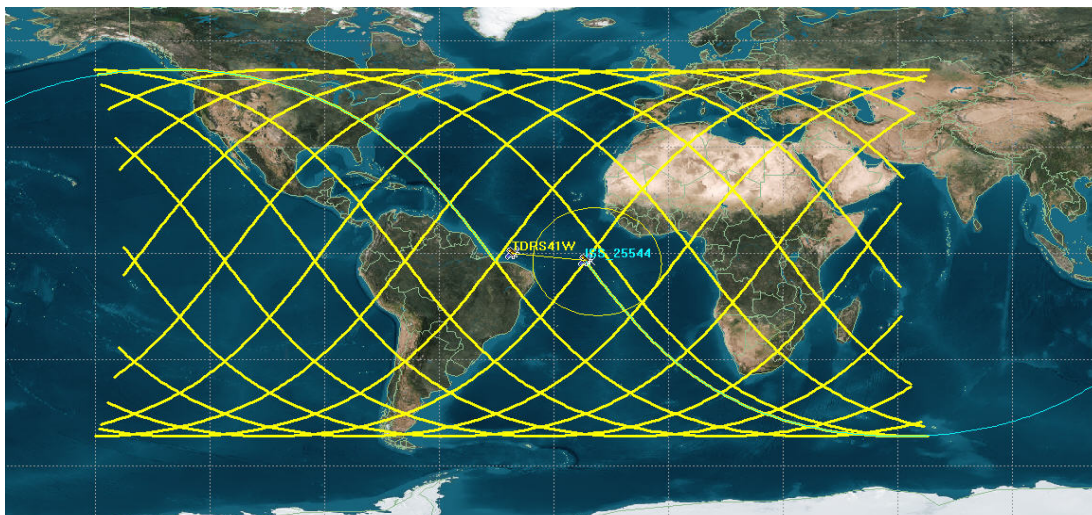


The geostationary location of TDRSS provides capability for satellites in lower orbits to have seamless communications with one or more earth stations. This is a critical requirement for space science missions and space exploration programs as data to and from low Earth orbiting satellites observing the Earth, performing scientific measurements, or receiving telecommand can be transmitted in real-time via TDRSS.

The analysis presented in this report on the sharing potential of the frequency band 2 025-2 110 MHz focuses exclusively on the forward links from the TDRS located at 41° West longitude to a few of NASA's satellites in low Earth orbit as a typical data relay operation. These forward links are critical because they are used for command and control of LEO satellites that collect data for weather prediction and science research. For example, the International Space Station forward link must be available for uninterrupted communication because it is used exclusively by astronauts for communications with earth stations and command centres.

The analysis presented in this report on the sharing potential in the frequency band 2 200-2 290 MHz focuses exclusively on the return links between ISS in low Earth orbit and the TDRS located at 41° West longitude as a typical data relay operation. As can be seen in Figure 2, the orbit of the ISS, while in communication with the TDRS at 41° West, places it above a variety of locations around the Earth. The ISS to TDRS links was used in these analyses because the return links used by the ISS astronauts is critical and must be available for uninterrupted communication to ground stations while the ISS is orbiting the Earth. Further, the ISS uses the TDRSS almost exclusively for communications to earth stations and command centres. With regards to the forward link analysis as discussed in the report, the track of the ISS as shown in Figure 2 is typical of many of the satellites considered in the analysis.

FIGURE 2
Overview of ISS beam track over a 24 hour period



This report focuses on one orbital location of the TDRS, however similar results would be obtained for other TDRS orbital locations because each TDRS has similar parameters. Further, other DRSs operated by China (CTDRS), ESA (ARTEMIS), Japan (DRTS), and Russia (CSDRN-M/ VSSRD-2M/ WSDRN-M) have notified frequency assignments across the 2 025-2 110 MHz and 2 200-2 290 MHz frequency band. These DRS systems can also be expected to have similar results as those presented for TDRS 41° West because their return links have characteristics similar to those of TDRS, as can be seen in Recommendation ITU-R SA.1414. Recommendation ITU-R SA.1275 specifies orbital locations for DRS systems in the 2 200-2 290 MHz frequency band. *Recommends 1* from Recommendation ITU-R SA.1275 states: "that receivers on-board DRS that operate in the 2 200-2 290 MHz frequency band which should be protected in accordance with Recommendation ITU-R F.1247 are located in the following geostationary orbital positions (given in the East direction): 10.6°, 16.4°, 16.8°, 21.5°, 47°, 59°, 77°, 80°, 85°, 89°, 90.75°, 95°, 113°, 121°, 133°, 160°, 167°, 171°, 176.8°, 177.5°, 186°, 189°, 190°, 192.5°, 198.5°, 200°, 221°, 281°, 298°, 311°, 314°, 316°, 319°, 328°, 344°, 348°." (Note that 319°E = 41°W).

2.1.1 TDRSS protection criteria and applicable ITU-R Recommendations

The protection criteria used in the analyses considered in this document, as specified in Recommendation ITU-R SA.1154, is an aggregate interfering signal power density from mobile systems in the frequency bands 2 025-2 110 MHz and 2 200-2 290 MHz of -184 dB (W/kHz) at the DRS receiving antenna port, not to be exceeded for more than 0.1% of the time. Applicable recommendations listing orbital locations and characteristics of data relay satellites include:

- Recommendation ITU-R SA.1414 - Characteristics of data relay satellite systems;
- Recommendation ITU-R SA.1275 - Orbital locations of data relay satellites to be protected from the emissions of fixed service systems operating in the band 2 200-2 290 MHz and hence the 2 025-2 110 MHz band since it is a companion to the 2 200-2 290 MHz band;
- Recommendation ITU-R SA.1155 - Protection criteria related to the operation of data relay satellite systems.

2.2 Commercial broadband LTE systems

The wireless broadband technologies systems analysed at 2 025-2 110 MHz and 2 200-2 290 MHz were assumed to implement LTE technology with parameters that were provided in Report ITU-R M.2292 for use in sharing studies under WRC-15 agenda item 1.1. Although this analysis assumes wireless broadband characteristics based on the LTE technology standard, the results would also apply to other types of wireless broadband technology with similar characteristics.

3 Technical characteristics

This section provides the technical characteristics of the space-to-space forward and return links and the commercial broadband systems that were used for this sharing study. Section 3.1.1 provides the technical characteristics of the space-to-space links from the TDRS located at 41° West to some of NASA typical user satellites. Section 3.1.2 provides the technical characteristics of the space-to-space links from the ISS transmitting to a TDRS located at 41° West. Section 3.2 provides the technical characteristics for the commercial mobile broadband base-stations and user equipment (UE) terminals. Additional technical characteristics used for these sharing analyses can be found in the Appendices.

3.1 Technical characteristics for space-to-space links used in the analysis

3.1.1 Space-to-space forward links

The forward links considered in this analysis are from TDRS 41° West to the systems listed in Table 1.

When calculating the interference into the forward links, it was assumed that:

- the receiver technical characteristics as listed in Table 1;
- the receiver antenna pattern used is Recommendation ITU-R S.672 (first sidelobe is 25 dB down from the peak);
- the polarization discrimination is 3 dB on and off-axis (Circular polarized forward links vs. LTE linear polarization);
- the ITU-R recommended threshold is threshold for Interference from mobile System Transmitters: $I_o = -184$ dBW/kHz to be exceeded no more than 0.1% of the time per Recommendation ITU-R SA.1154, *recommends* 1.2.

TABLE 1
TDRS user satellite receiver technical characteristics

Receiver	Altitude (km)	Inclination (degrees)	Eccentricity	Min. Frequency (MHz)	Max. Frequency (MHz)	Antenna Gain (dBi)	System Noise Temp. (K)
Cygnus	460	51.6	0.000	2037.49	2043.65	1.6	1849
GPM	407	65.0	0.000	2103.33	2109.49	23.0	226
ISS - LGA	400	51.6	0.000	2082.61	2088.77	1.1	479
TERRA	705	98.2	0.000	2103.33	2109.49	25.8	410
TRMM - HGA	403	35.0	0.001	2073.86	2080.02	23.0	513

3.1.2 Space-to-space return links

The TDRSS technical system characteristics used in these analyses are indicated in Tables 2 and 3 below.

TABLE 2
TDRSS technical characteristics

System	Parameter	Value
TDRSS Inter-Orbit Return Link Satellite at 41° West	Rx Antenna Gain & Polarization	36.6 dBi, circular
	Polarization Discrimination	3 dB on- and off-axis (vs LTE linear polarization)
	Rx Antenna Pattern <i>Recommendation ITU-R SA.1414</i>	As specified in Rec. ITU-R S.672-4 (LS = -25)
	Interference threshold for mobile Transmitters <i>Recommendation. ITU-R S.1154</i>	I = -184 dB(W/kHz) to be exceeded for no more than 0.1% of the time
	DRS return link receiver noise power (N)	N = -170.7 (dBW/(kHz))
	Interference-to-Noise Power Ratio	I/N = -13.3 dB not to be exceeded for more than 0.1% of the time

TABLE 3
ISS transmit link technical characteristics

System	Parameter	Value
ISS Transmit Link 400 kilometres Orbit at 51.6 degree inclination	Tx Antenna Gain	0 dBi, Omni

3.2 Commercial broadband LTE parameters

As discussed in section 2.2, the technical parameters for commercial broadband LTE systems were provided in Report ITU-R M.2292 for the sector antenna pattern in Recommendation ITU-R F.1336 as specified in that Report, see Appendix C. The technical parameters used in the analyses were varied to test a range of assumptions. The assumptions regarding base-station resource loading, power distributions, clutter and other propagation losses, were varied so as to encompass a range of assumptions that are associated with worst-case and best-case frequency sharing scenarios. Section 3.2.1 provides an overview of technical characteristics for LTE base-stations and section 3.2.2 provides an overview of technical characteristics for LTE user equipment (UE). Further, more detailed parameters such as aggregate base-station and user equipment e.i.r.p. calculation methods, deployment models, antenna patterns, and a listing of cities used in the analyses can be found in the appendices.

3.2.1 Overview of LTE base-station technical parameters

The LTE base-station technical parameters are presented in Table 4 and an overview of the deployment model is presented in Table 5 and Figures 3 and 4. The transmit power values shown in Table 4 are levels emanating from LTE ground transmissions.

TABLE 4
LTE base-station technical characteristics

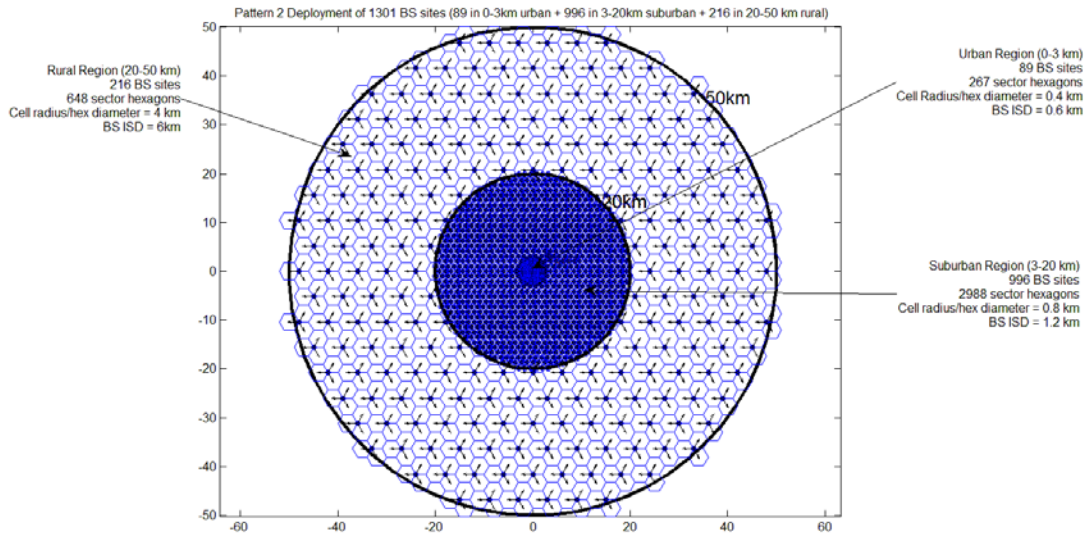
LTE base-station Parameter	Parameter
Antenna Pattern	Sector antenna (Recommendation ITU-R F.1336, <i>recommends</i> 3.1, see Appendix C)
Sector antenna pointing azimuth	120 degree spacing on the same tower; randomly oriented among towers (relative to true north)
Sector antenna pointing elevation	10 degrees down tilt for each urban zone sector antenna 6 degrees down tilt for each suburban zone sector antenna 3 degrees down tilt for each rural zone sector antenna
Sector antenna height	10 meters (AGL)
Sector antenna gain	16 dBi (ITU-R antenna) for each urban and suburban zone sector antenna 18 dBi (ITU-R antenna) for each rural zone sector antenna
Sector transmit power (Recommendation ITU-R F.1336-3 antenna)	Peak power of 40W/10 MHz with 50% and 20%, time-frequency resource loading depending on interference scenario
Net Power per city zone	See Appendix B Urban Zone : 29.44 dBW (50% loading), 25.47 dBW (20% loading) Suburban Zone : 43 dBW (50% loading), 39 dBW (20% loading) Rural Zone : 36.35 dBW (50% loading), 32.38 dBW (20% loading)
LTE channel bandwidth	10 MHz
Elevation mask for Recommendation ITU-R F.1336-3	Three cases: hypothetical complete site shielding of signals on paths having elevation angles below 0, 20, 45 degrees

TABLE 5
LTE base-station deployment model

Deployment scenario	Value
Analyses city deployment	160 large cities with population greater than 250,000 (see Appendix E)
LTE base-station deployment)	- Urban zone extends out 0-3 kilometres from city centre and contains 89 base-station sites (0.6 kilometres ISD) - Suburban zone extends 3-20 kilometres from city centre and contains 996 base-station sites (1.2 kilometres ISD) - Rural zone extends from 20-50 kilometres from city centre and contains 216 base-stationsites (6 kilometres ISD)

FIGURE 3

LTE base-station deployment for 160 large cities



3.2.2 Overview of LTE user equipment (UE) technical parameters

The UE technical characteristics are presented in Table 6. Please refer to Appendix A for the derivations of the aggregate total e.i.r.p. levels for cities. The aggregate, per-city e.i.r.p. level is the total e.i.r.p. from all UE located in the city (Figure 3 or 4) which is assumed to be emanating from the centre of the city, as further explained in section 4 and Appendix A.

TABLE 6

LTE user terminal technical characteristic

Technical characteristic	Value
Net Aggregate Power per UE city zone	Urban Zone : 39.96 dBm Suburban Zone : 51.48 dBm Rural Zone : 48.71 dBm
Antenna Pattern	Omni Directional
Cellular Deployment Scenario	Same as LTE base-stations presented in section 3.2.1

4 Analysis

This section presents the results of the sharing feasibility assessment conducted between the TDRSS return links and commercial broadband LTE operations in the frequency bands 2 025-2 110 MHz and 2 200-2 290 MHz. For these analyses of sharing feasibility, software was used to model the dynamic interference situations. The TDRS 41° West location was selected as a representative DRS location operating with return links of the ISS. Interference from the LTE system was simulated using a cellular distribution around selected worldwide cities using technical parameters as discussed in section 3.2. The analyses considered potential interference from base-station to UE emissions and UE to base-station emissions.

In the particular case of interference analysis to the TDRS forward links in the frequency band 2 025-2 110 MHz, at each time sample, which was selected randomly, potential interference into the TDRS user is calculated from the aggregate of LTE interferers. In the particular case of interference analysis to the TDRS return links in the frequency band 2 200-2 290 MHz, potential interference into the TDRS was calculated from the aggregate of LTE interferers every 10 seconds as the TDRS receiver tracked the ISS for a period long enough to obtain stable results. This varied from 14 to 30 days.

For the purposes of reduced computational complexity, the aggregate power from each base-station distribution zone (i.e. urban, suburban, rural) was assumed at the city centre. The power for all UE transmissions was aggregated at the centre of each city in the simulation. The method for calculating the aggregate power per city for LTE UEs is presented in Appendix A. The method for calculating aggregate LTE base-station power for cities is presented in Appendix B.

Figure 4 presents an overview of TDRSS operations and the potential for interference as studied in the analysis for the frequency band 2 025-2 110 MHz. The analysis presented in this document on these frequency bands considers interference paths to the TDRSS forward links as shown in Figure 4.

Figure 5 presents an overview of TDRSS operations and the potential for interference as studied in the analyses for the frequency band 2 200-2 290 MHz. As can be seen in the figure, the analyses presented in this document for these frequency bands consider interference paths to the TDRSS return links while receiving a transmission from the ISS.

Figure 6 presents an overview of the TDRS 41°W receiver antenna main beam coverage while tracking the ISS over a 24 hour period. As can be seen, the TDRS beam is wide enough to cover significant portions of continents and multiple LTE deployment cities over any instant in time.

Section 4.1.1 presents results of potential interference to TDRSS return links from LTE base-stations in the frequency band 2 025-2 110 MHz and section 4.1.2 presents the results of the same analyses in the frequency band 2 200-2 290 MHz. Section 4.2.1 presents results of potential interference to TDRSS return links from LTE user terminals in the frequency band 2 025-2 110 MHz and section 4.2.2 presents the results of the same analyses in the frequency band 2 200-2 290 MHz.

FIGURE 4

Overview of interference analysis into TDRS system in the 2 025-2 110 MHz frequency band

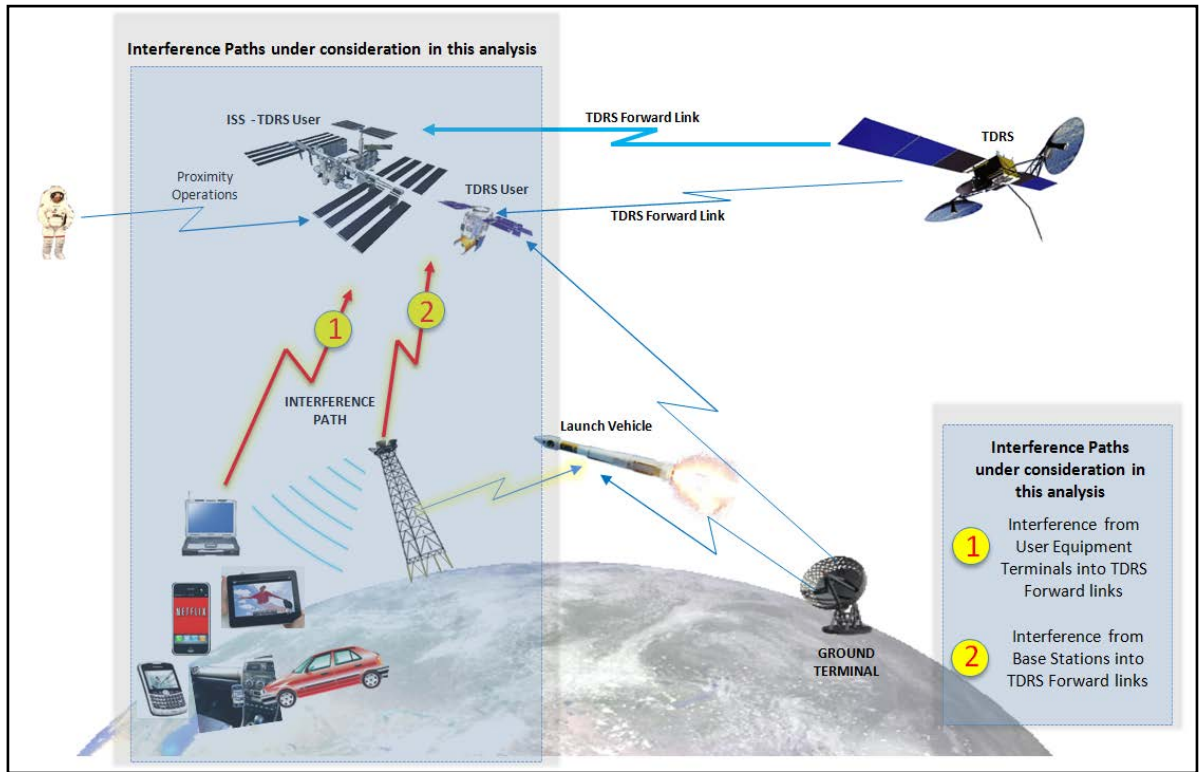


FIGURE 5

Overview of sharing analyses conducted into TDRS operations in the 2 200-2 290 MHz frequency band and interference paths considered

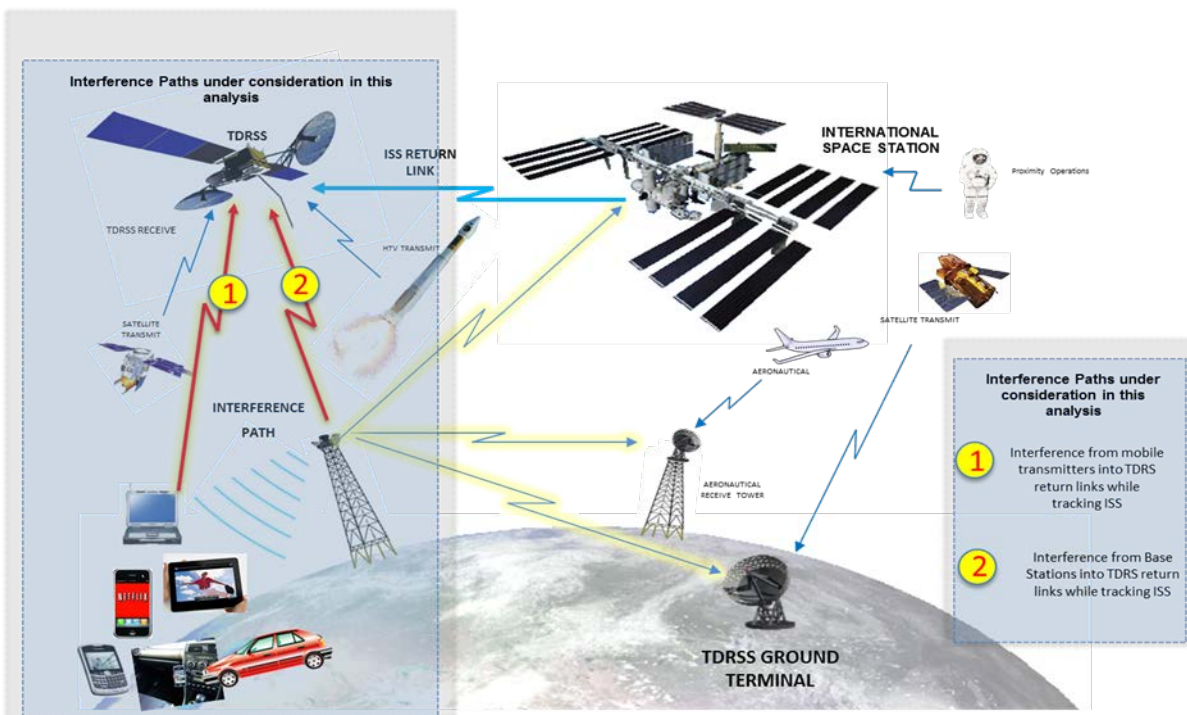
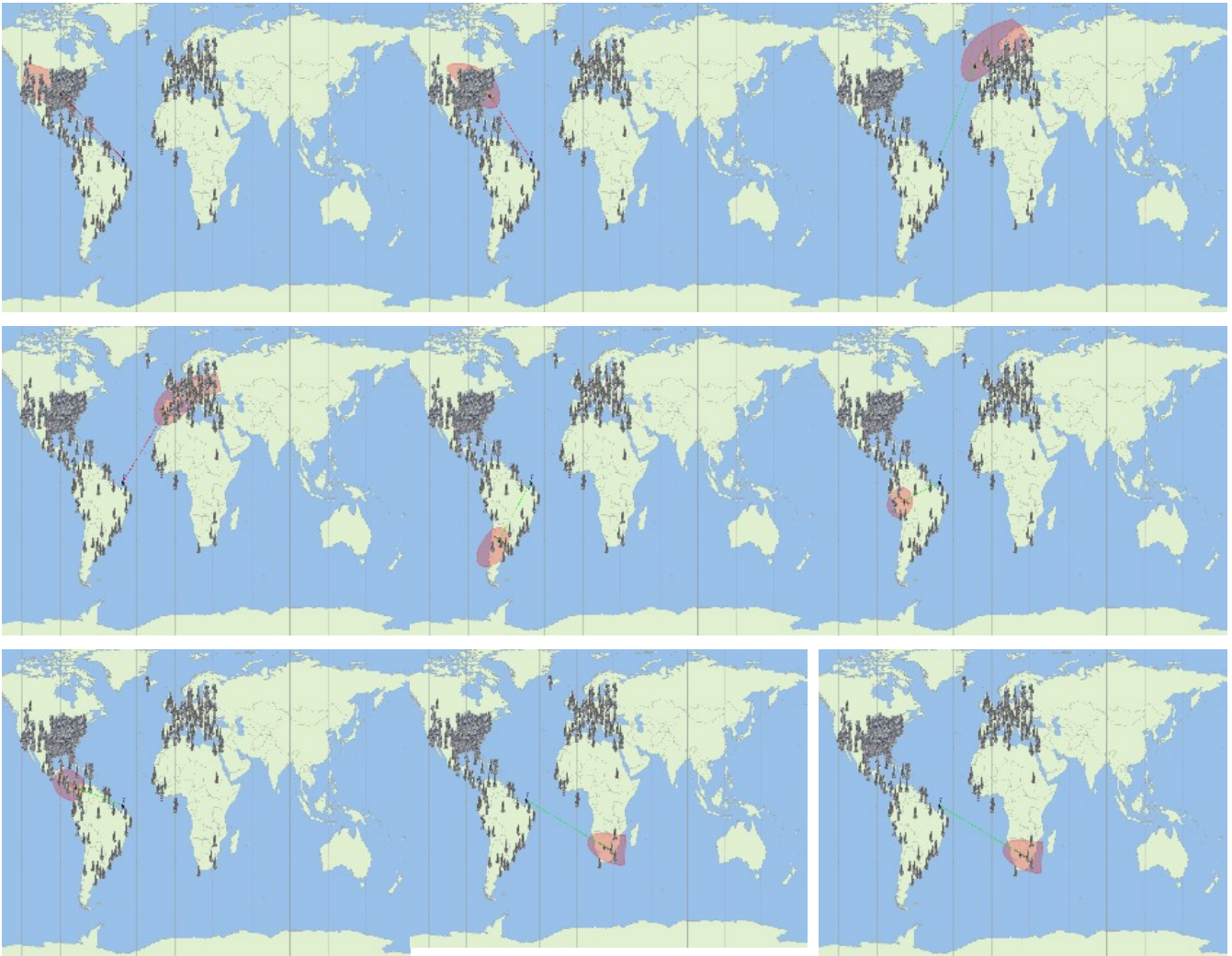


FIGURE 6

Overview of TDRS 41-W beam coverage over a 24 hour period while tracking the ISS



The LTE deployment model considered in these analyses assumed no base-stations more than 50 kilometres from the centre of each city. In large metropolitan areas, it is likely that there will be deployments outside of the 50 kilometres cut off considered in these analyses. The LTE base-stations in these analyses assumed a peak output power value of 40 W/10 MHz. However, the LTE base-station standards contain no power limits. Some other assumptions favouring sharing were low base-station resource loading, and complete blockage of interfering signal paths based on the elevation angle from the city to the satellite due to shielding. Within the urban zones, Report ITU-R M.2292 specifies that 50% of the base-stations are below building roof tops. It was assumed in the analysis that none of the base-stations below building roof tops contributed any interference. Further, for the analyses involving UE transmissions, Report ITU-R M.2292 specifies that 70% of UE's in the urban and suburban zone and 50% of UE's in the rural zone are to be assumed indoors. In the analyses all indoor UE's were excluded from contributing to the interference. In addition to the elevation angle based shielding blockages, an additional clutter loss for the UE transmissions was considered for every city. This clutter loss was based on Recommendation ITU-R P.452 § 4.5.3, where the clutter attenuation was calculated using a set of clutter categories from the recommendation.

The maximum elevation angle for the interfering clutter path was then calculated for each city and the appropriate clutter loss was applied to each city (see Appendix D). Lastly, the analyses considered LTE deployment in only 160 worldwide cities within view of TDRSS at 41W, whereas a full deployment of LTE systems will involve many more cities that will be in view of the TDRS antenna beam.

The analysis approach used herein can be generalized to consider other sharing scenarios. The cumulative probability distributions (CDFs) of aggregate interfering signal power levels presented below in this document (Figures 8-11) can in many cases be shifted upward or downward to estimate the effects of alternative assumptions that have not been addressed in this study. For example, the aggregate UE and base-station e.i.r.p. per-city values are key intermediate results that encompass the effects of several assumed IMT equipment operating parameters.

4.1 Potential interference from LTE base-stations

4.1.1 Potential interference from LTE base-stations in the frequency band 2 025-2 110 MHz

Table 7 and Table 8 present the results of analysis considering the potential for sharing with LTE base-stations. This analysis considered base-station transmitters using the antenna pattern of Recommendation ITU-R F.1336, *recommends* 3.1 (See Appendix C) for the base-station sector antennas. In each case, several loading scenarios were modelled. The analysis considered a shielding factor, which assumed full signal blockage at elevation angles below 0°, 20°, and 45° between the base-station and the TDRS user in order to consider hypothetical best- and worst-case scenarios (e.g. a 20° elevation mask means that only LTE base-stations, which have visibility with the TDRS user satellite above 20° contribute to the aggregate interference at a given time sample). From each table of results, one forward link was chosen - GPM Forward Link - to show the cumulative density function (CDF) curve (Figure 7,) which demonstrated even at high percentage of the time (approaching or exceeding 10%) the ITU Io/No threshold criterion will not be met for all cases. Base-station heights are above clutter heights in suburban and rural zones. As mentioned previously all base-stations below roof tops in urban zones (50%) were completely excluded from the analysis (i.e. complete blockage was assumed for base-stations below urban rooftops).

TABLE 7

Potential interference from the base-stations (Recommendation ITU-R F.1336 antenna) into typical NASA TDRS forward links with 20% time-frequency resource loading

Visibility Elevation Mask (deg)				0 degrees		20 degrees		45 degrees	
User Spacecraft	SNT (K)	No (dBW/Hz)	Io/No threshold (dB)	I/N (dB) @ 0.1%	Exceedance (dB)	I/N (dB) @ 0.1%	Exceedance (dB)	I/N (dB) @ 0.1%	Exceedance (dB)
TERRA	410	-202.47	-11.53	32.5	44.03	21.4	32.93	18.1	29.63
Cygnus	1849	-195.93	-18.07	20.2	38.27	15.5	33.57	11	29.07
GPM	226	-205.06	-8.94	37.3	46.24	26.5	35.44	21.8	30.74
ISS-LGA	479	-201.80	-12.20	25.7	37.90	21.3	33.50	16.9	29.10
TRMM-HGA	513	-201.50	-12.50	37.6	50.10	22.1	34.60	18.3	30.80

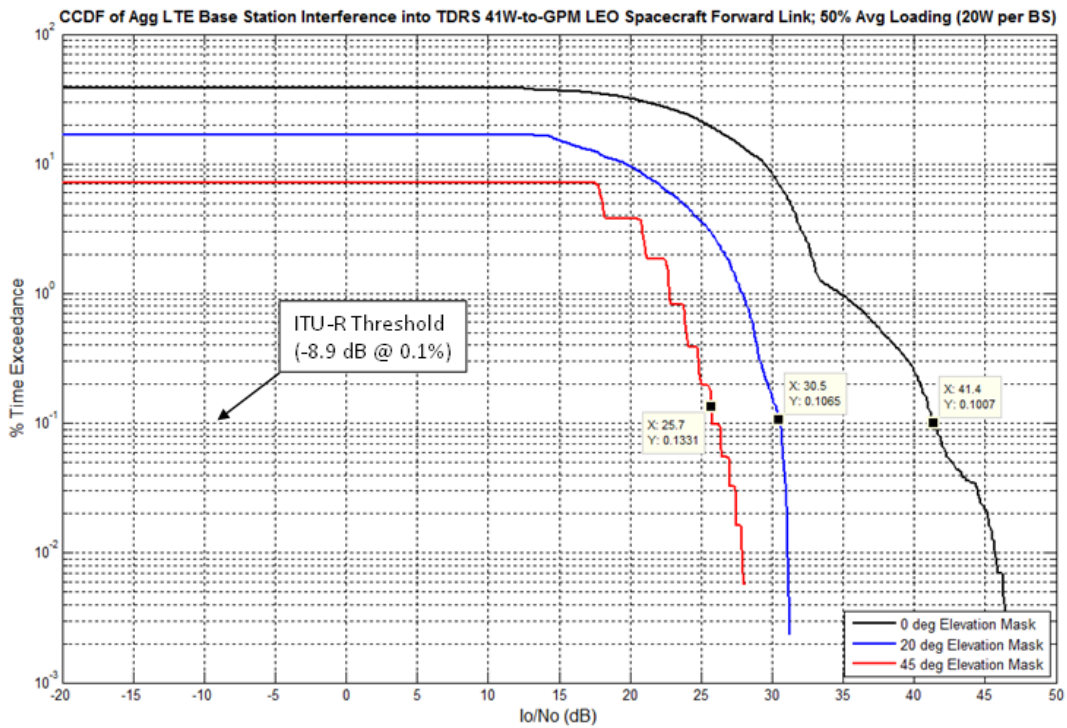
TABLE 8

Potential interference from the base-stations (Recommendation ITU-R F.1336 antenna) into typical NASA TDRS forward links with 50% time-frequency resource loading

Visibility Elevation Mask (deg)				0 degrees		20 degrees		45 degrees	
User Spacecraft	SNT (K)	No (dBW/Hz)	Io/No threshold (dB)	I/N (dB) @ 0.1%	Exceedance (dB)	I/N (dB) @ 0.1%	Exceedance (dB)	I/N (dB) @ 0.1%	Exceedance (dB)
TERRA	410	-202.47	-11.53	36.9	48.43	25.4	36.93	22.1	33.63
Cygnus	1849	-195.93	-18.07	24.2	42.27	19.5	37.57	15	33.07
GPM	226	-205.06	-8.94	41.4	50.34	30.5	39.44	25.7	34.64
ISS-LGA	479	-201.80	-12.20	29.6	41.80	25.2	37.40	20.9	33.10
TRMM-HGA	513	-201.50	-12.50	41.8	54.30	26.1	38.60	22.3	34.80

FIGURE 7

Potential interference from LTE base-stations into GPM forward link taking into account site shielding elevation mask



**4.1.2 Potential interference from LTE base-stations in the frequency band
2 200-2 290 MHz**

Table 9, Table 10 and Figure 8 present the results of analyses considering the potential for sharing with LTE base-stations in the frequency band 2 200-2 290 MHz. These analyses considered base-station transmitters using the antenna pattern of Recommendation ITU-R F.1336, *recommends* 3.1 (See Appendix C) for the base-station sector antenna. In each analysis, several loading scenarios, corresponding to the peak LTE base-station transmit power was modelled. The analysis considered a shielding model assuming full signal blockage at elevation angles below 0, 20, and 45 degrees between the base-station and the TDRS 41° West satellite in order to consider hypothetical best- and worst-case scenarios (e.g. a 20 degree elevation mask means that only LTE base-stations which have visibility to the 41° West TDRS satellite above 20 degrees contribute to the aggregate interference). Base-station heights are above clutter heights in suburban and rural zones. As mentioned previously, all base-stations below roof tops in urban zones (50%) were completely excluded from the analysis (i.e. complete blockage was assumed for base-stations below urban roof tops).

TABLE 9

Potential interference from base-stations (Recommendation ITU-R F.1336 antenna) using elevation mask clutter attenuation into typical NASA TDRS return links and 20% time-frequency resource loading

Visibility Elevation Mask (deg)	0 degrees		20 degrees		45 degrees	
	I/N (dB) @ 0.1%	Exceedance (dB)	I/N (dB) @ 0.1%	Exceedance (dB)	I/N (dB) @ 0.1%	Exceedance (dB)
	28.8	42.1	23.6	36.9	16.7	30

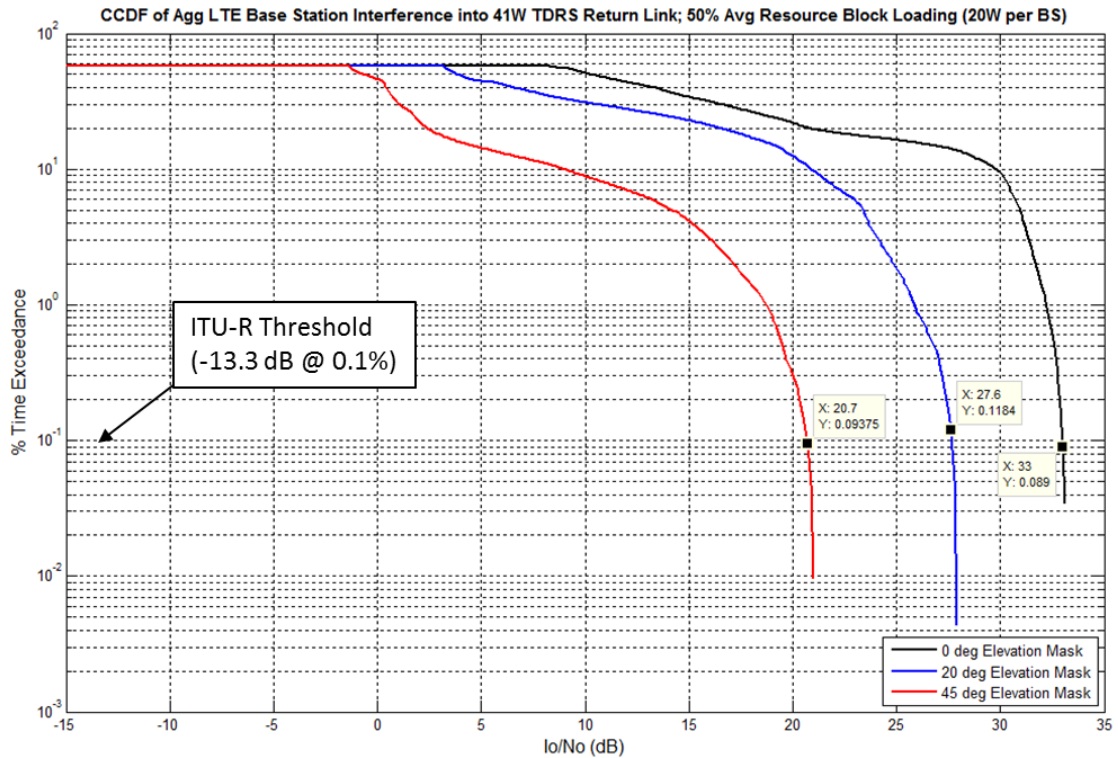
TABLE 10

Potential interference from base-stations (Recommendation ITU-R F.1336 antenna) using elevation mask clutter attenuation into typical NASA TDRS return links and 50% time-frequency resource loading

Visibility Elevation Mask (deg)	0 degrees		20 degrees		45 degrees	
	I/N (dB) @ 0.1%	Exceedance (dB)	I/N (dB) @ 0.1%	Exceedance (dB)	I/N (dB) @ 0.1%	Exceedance (dB)
	32.8	46.1	27.6	40.9	20.7	34

FIGURE 8

Potential interference from LTE base-stations into TDRS return link taking into account site shielding elevation mask



4.2 Potential interference from LTE user equipment

4.2.1 Potential interference from LTE user equipment in the frequency band

2 025-2 110 MHz

Table 11 presents the results of analysis considering the potential of sharing LTE user equipment distributed over cities worldwide with TDRS 41° West forward link transmissions to some typical NASA TDRS users in the frequency band 2 025-2 110 MHz. For this case, a hypothetical shielding mask was analysed for angles below 0°, 20°, and 45° in relation to the TDRS users (e.g. a 20° elevation mask means that only LTE UE location which have visibility to the TDRS user satellite above 20° contribute to the aggregate interference at a given time sample). Further, an additional clutter factor based on Recommendation ITU-R P.452 was considered in the analysis. Again, for illustrative purposes, one forward link was chosen (GPM) to show the CDF curve (Figure 9).

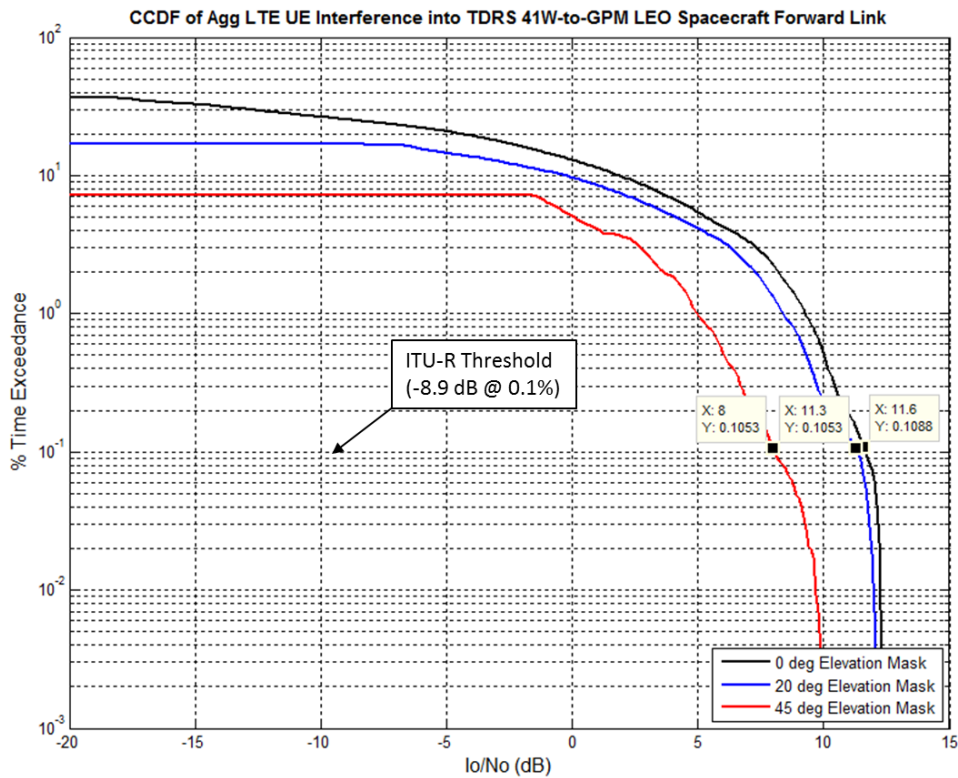
TABLE 11

Potential interference from LTE user equipment including elevation angle based shielding blockage and additional clutter loss based on Recommendation ITU-R P.452 into typical NASA TDRS forward links

Visibility Elevation Mask (deg)				0 deg		20 deg		45 deg	
User Spacecraft	SNT (K)	No (dBW/Hz)	Io/No threshold (dB)	I/N (dB) @ 0.1%	Exceedance (dB)	I/N (dB) @ 0.1%	Exceedance (dB)	I/N (dB) @ 0.1%	Exceedance (dB)
TERRA	410	-202.47	-11.53	6.7	18.23	6.4	17.93	4.2	15.73
Cygnus	1849	-195.93	-18.07	0.5	18.57	-0.2	17.87	-3.1	14.97
GPM	226	-205.06	-8.94	11.6	20.54	11.3	20.24	8	16.94
ISS-LGA	479	-201.80	-12.20	6.3	18.50	5.7	17.90	2.7	14.90
TRMM-HGA	513	-201.50	-12.50	7.2	19.70	6.5	19.00	4.1	16.60

FIGURE 9

Potential Interference from the LTE user equipment terminals into GPM Forward Link taking into account site shielding mask and additional clutter based on Recommendation ITU-R P.452



4.2.2 **Potential interference from LTE user equipment in the frequency band
2 200-2 290 MHz**

Table 12 and Figure 10 presents the results of analyses considering the potential of sharing LTE user equipment distributed over worldwide cities with TDRS 41° West return links receiving a transmission from the ISS. For these analyses, a hypothetical full blockage shielding mask was analysed for those cities having elevation angles below 0 degrees, 20 degrees, and 45 degrees in relation to the TDRS 41° West (e.g. a 20 degree elevation mask means that only LTE user equipment which have visibility to the 41° West TDRS satellite above 20 degrees contribute to the aggregate interference). Further, an additional clutter factor based on Recommendation ITU-R P.452 was considered in the analysis.

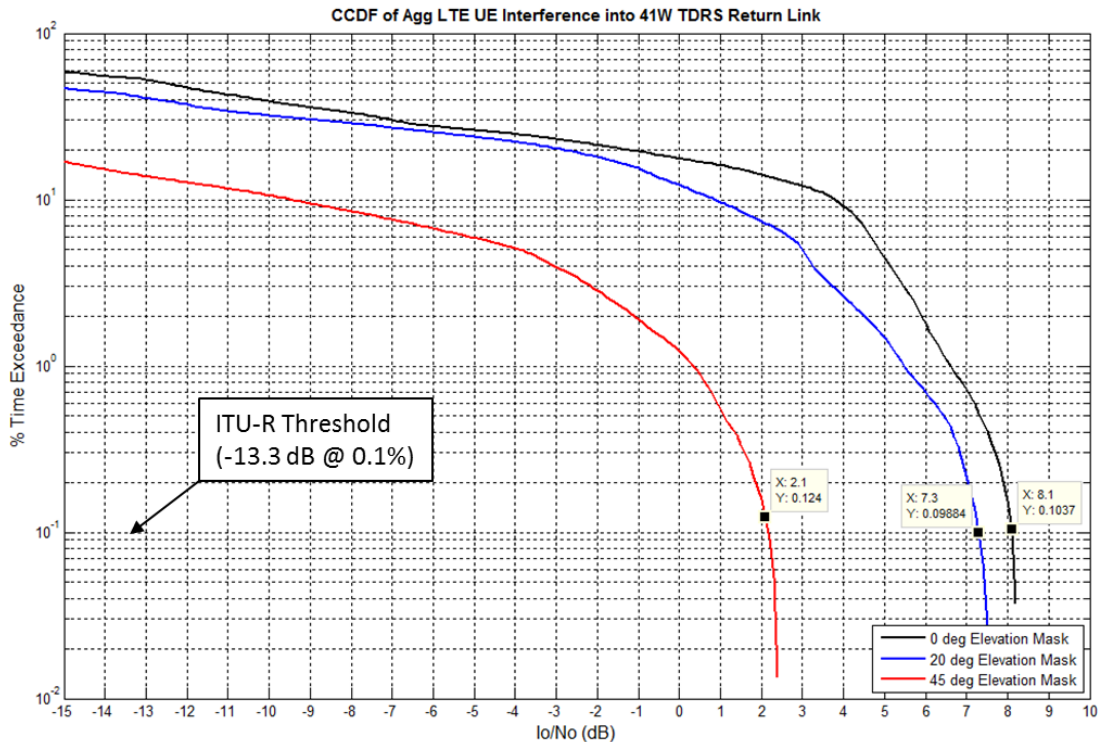
TABLE 12

Potential interference from the LTE user equipment terminals using elevation mask shielding and additional clutter attenuation based on Recommendation ITU-R P.452 into typical NASA TDRS return links

Visibility Elevation Mask (deg)	0 degrees		20 degrees		45 degrees	
	I/N (dB) @ 0.1%	Exceedance (dB)	I/N (dB) @ 0.1%	Exceedance (dB)	I/N (dB) @ 0.1%	Exceedance (dB)
	8.1	21.4	7.3	20.6	2.1	15.4

FIGURE 10

Potential interference from LTE user terminals into TDRS return links taking into account elevation angle based site shielding and additional clutter loss based on Recommendation ITU-R P.452



5 Summary

This document presents study results on the feasibility of sharing with DRS (space-to-space) forward link and return link operations between typical TDRSS users and the TDRSS in the frequency bands 2 025-2 110 MHz and 2 200-2 290 MHz.

Interference scenarios were considered between the DRS return link operations and a worldwide LTE deployment in 160 highly populated world cities (see Appendix E for a list of cities). LTE uplink and downlink operations that were considered included either transmitting base-station or transmitting user equipment, but not both simultaneously. LTE base-station and user equipment parameters used in these analyses were provided in Report ITU-R M.2292 and the base-station sector antenna pattern was provided in Recommendation ITU-R F.1336 Annex C. The assumptions and parameters used in the analyses such as LTE deployment models transmit power, shielding, clutter loss, and propagation conditions were varied in order to analyse a range of scenarios. Although this analysis assumes wireless broadband characteristics based on the LTE technology standard, the results would also apply to other types of wireless broadband technology with similar characteristics.

The parameters used in the analyses were varied to test a range of assumptions. However, even with the wide range of parameters and very favourable sharing assumptions used for the analyses in this report, it can be seen that the level of interference exceeds the permissible criteria by so much that additional interference mitigations cannot sufficiently reduce interfering signal levels to enable sharing.

6 Conclusion

As can be seen from the analysis results it is found that sharing is not feasible between LTE systems and incumbent DRS forward and return links operating in the 2 025-2 110 MHz and 2 200-2 290 MHz frequency bands in the space research (space-to-space), Earth exploration-satellite (space-to-space) and space operations (space-to-space) services.

APPENDIX A

Method for calculating aggregate power per city zone for LTE UEs

This Appendix describes the methodology used to compute aggregate UE power for the urban/suburban/rural zones used in the simulations. It is based in part on the Monte Carlo simulation algorithm as presented below.

Figure A1 shows the (large) city LTE cell pattern layout assumed in the analysis. This cell pattern is deployed around each of the 160 cities used in the simulations.

FIGURE A1
LTE Cell Deployment Pattern

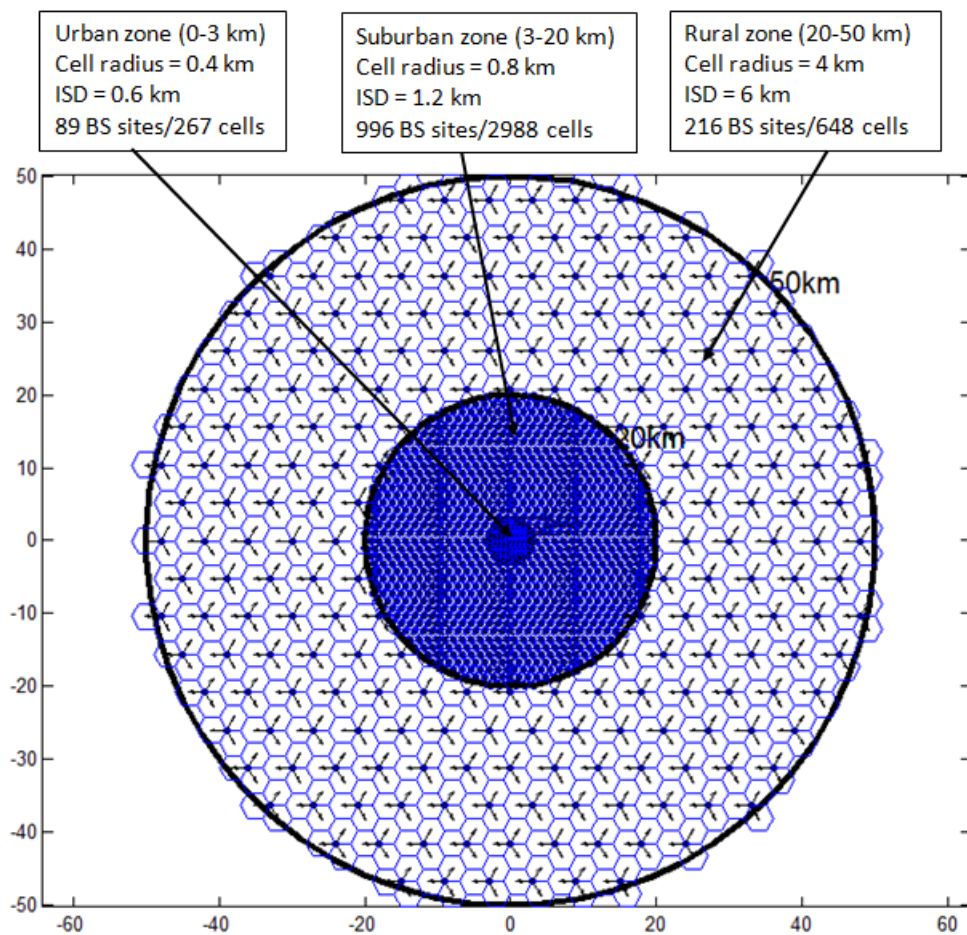
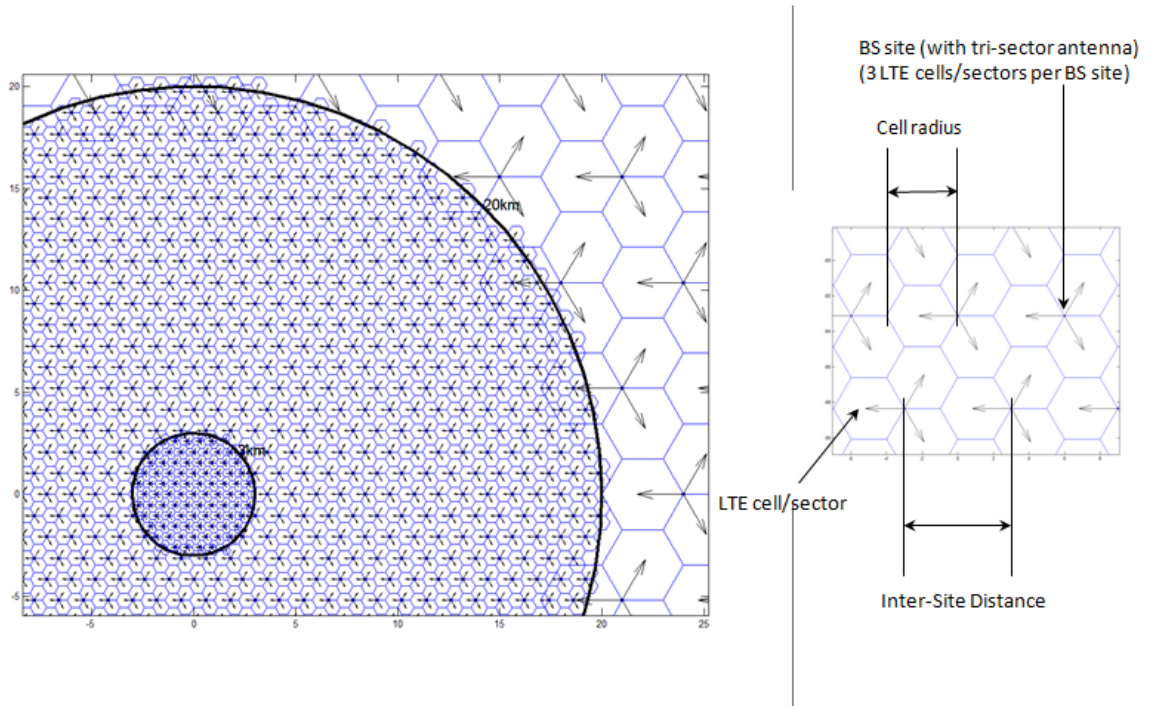


Figure A2 shows a close-up of the cell pattern and the definitions of cell radius and inter-site distance.

FIGURE A2
Close-up of LTE Cell Deployment Pattern



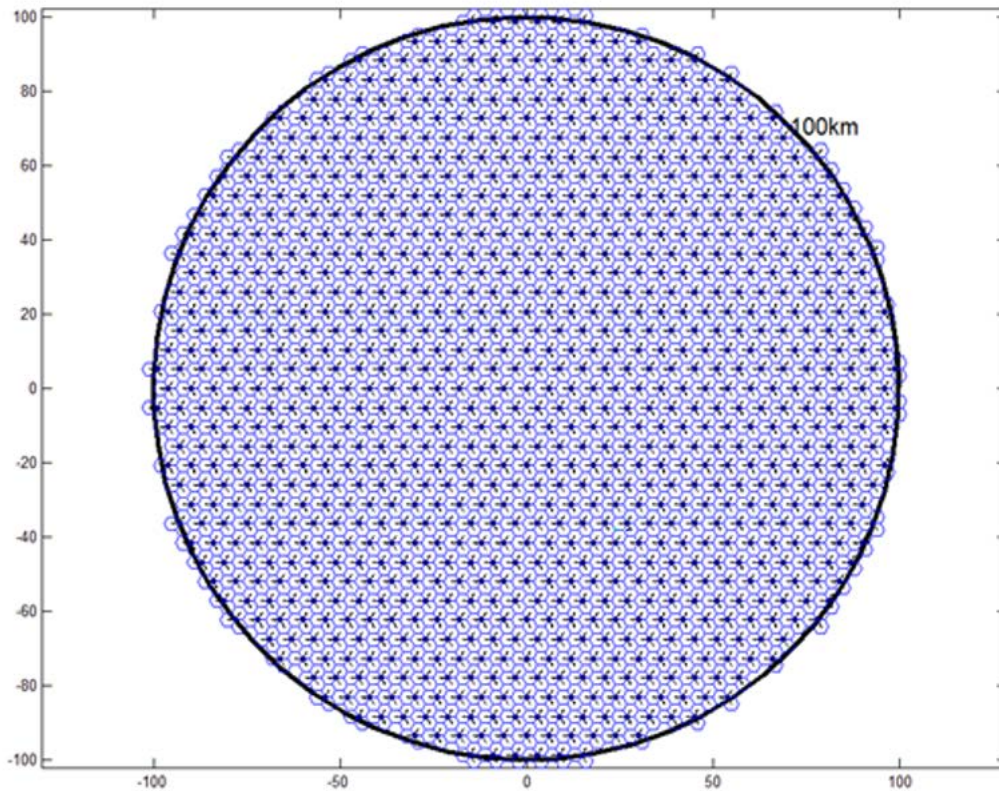
Note there are a total of 1301 base-station sites in the pattern (89 urban + 996 suburban + 216 rural) and a total of $3 \times 1301 = 3\,903$ cells. Assuming a world-wide city deployment of 160 major cities (i.e. cities with population > 250,000), the total number of cells in the scenario is then $160 \times 3\,903 = 624\,480$. The simulations involve calculating the aggregate interference from these LTE cells over a 10-day simulation period at 1-sec time steps (i.e. 864 000 time samples). Therefore, assuming 6 active UEs per cell, this represents a total of $624\,480 \times 864\,000 \times 6 = 3.24$ trillion UE calculations. Sample MATLAB simulations with these parameters required approximately 15 hours of run-time. To reduce simulation time, the aggregate UE interference was modelled by assuming (3) “effective” UEs per city – one for urban zone, one for suburban zone, and one for rural zone with all (3) effective UEs co-located at the city centre. Comparison of simulation results using this effective UE approach vs the full cell approach has demonstrated that this is a valid simplifying assumption since the results of the aggregate interference at the satellite in both cases are virtually identical (even for the lower altitude satellites assumed in the TDRSS forward link analysis). Therefore, the remainder of this Appendix will describe the calculation steps of the aggregate UE transmit power of the effective UEs in the urban, suburban, and rural zones. The same steps are used to find the aggregate power of the effective UE in each of the 3 zones.

Step 1

Fill up a large circular region with LTE cells of the specified cell radius and find the number of base-station sites in the region. For example, for the rural zone with a 4 kilometres cell radius, we fill up a 100 kilometres radius circular region with 4 kilometres cells as shown in Figure A3. In this case there are a total of 1 015 base-station sites/3 045 cells.

FIGURE A3

100-kilometres radius circular region filled with 4-km radius LTE cells

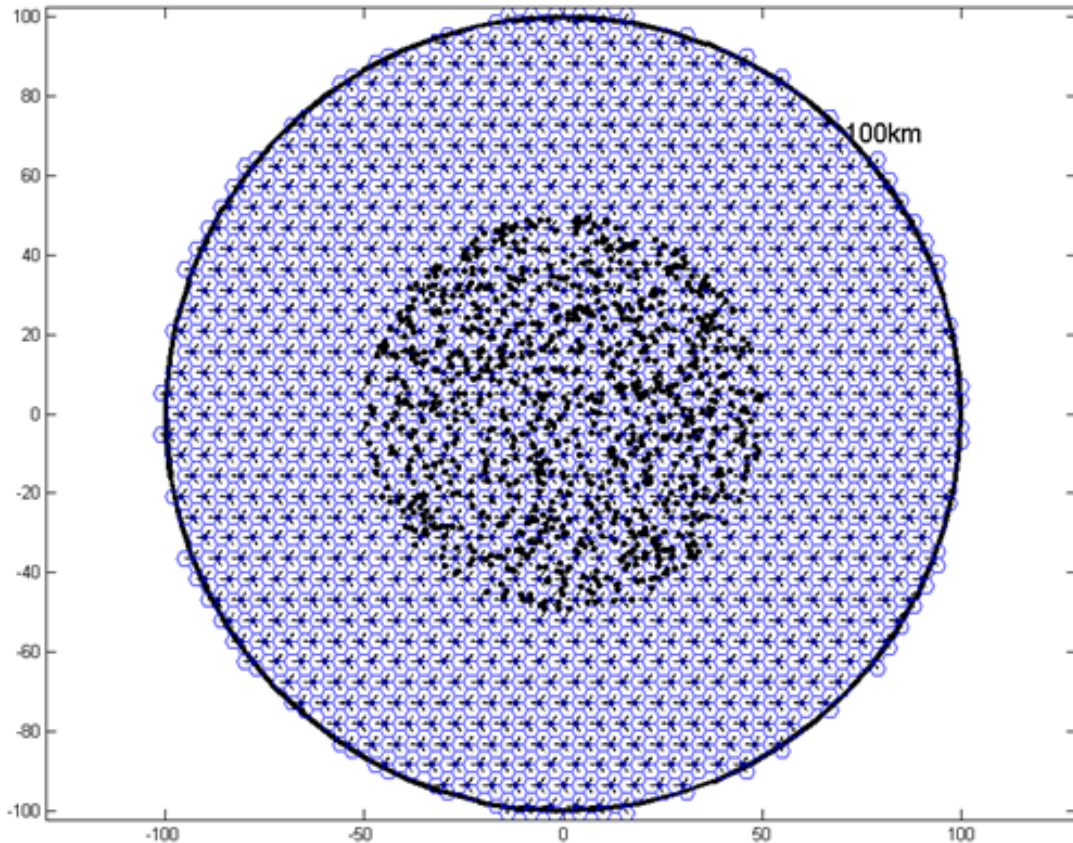


Step 2

For a large number of trials, perform the following procedure. For the i th trial, uniformly distribute a large number of UEs over a smaller region inside the larger region of cells. This is to allow UEs on the boundary of the smaller region to possibly be assigned to base-station outside the boundary of the smaller region so as not to skew the path loss (PL) distribution. For example, Figure A4 shows 1 000 UEs randomly uniformly distributed over a 50 kilometres radius region inside the 100 kilometres radius region of Figure A3.

FIGURE A4

Uniform distribution of 1000 UEs within 50 kilometres region inside 100 kilometres region



Step 3

Compute distance and PL between each UE and base-station site (using modified Hata propagation model in Report ITU-R SM.2028-1, Appendix 1 to Annex 2). For example, for 1 015 base-station sites and 1 000 UEs, this results in a PL matrix of size [1 000 x 1 015].

Step 4

For each UE find the minimum PL (PL_{\min}) and the base-station site associated with PL_{\min} . For example, for 1 000 UEs and 1 015 base-station sites, we generate a vector of 1 000 elements whose values are in the range 1-1015, indicating that for the i th UE ($i = 1$ to 1 000), the min PL is to the n th base-station site ($n = 1$ to 1 015).

Step 5

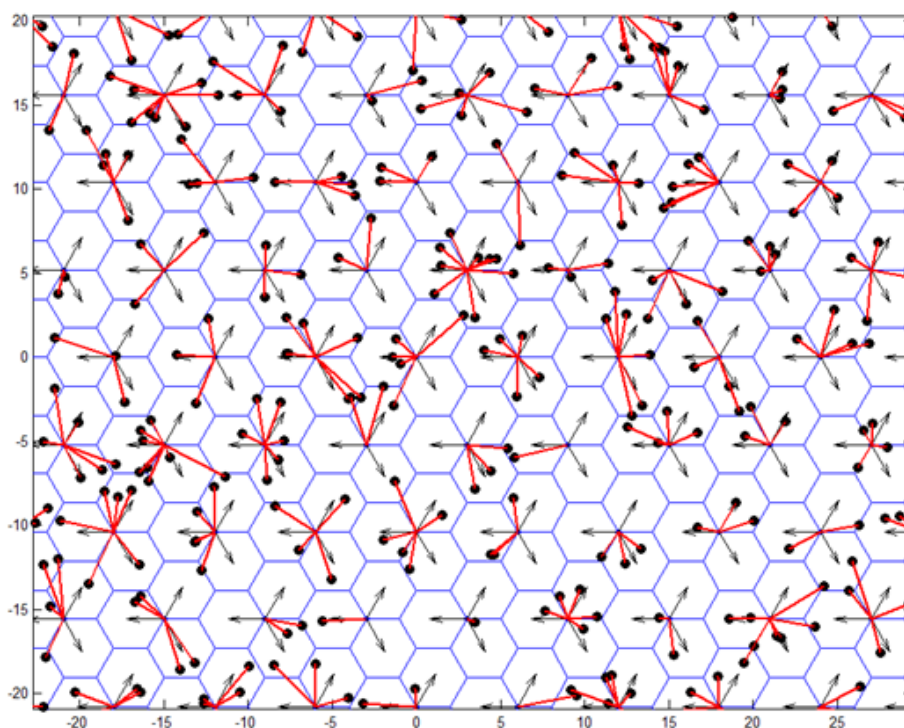
Now for each UE find the *subset* of base-station sites for which the PL $\leq (PL_{\min} + \text{HO margin})$ where HO margin is the HandOver margin (here assumed to be 3 dB). The HO margin is a predetermined value used to establish for each UE the set of LTE cells which that UE can connect to, besides the one with the strongest downlink received pilot power. Therefore, the UE (particularly those at the cell edges) may not always connect to the physically nearest base-station site.

Step 6

For each UE, randomly link it to one of the base-station sites from its corresponding subset of base-station sites (i.e. those base-station sites for which $PL \leq PL_{\min} + \text{HO margin}$). This will be its assigned base-station site.

For example, see Figure A5.

FIGURE A5
UEs Linked to Assigned base-stations



Step 7

For each UE, compute the PL (again using modified Hata) between it and its assigned base-station and add PL value to sample PL vector.

Step 8

Repeat steps 2-7 for a large number of trials in order to obtain a large PL sample vector (e.g. 1 million PL samples).

Step 9

Use the PL sample vector to generate the CDF (Cumulative Distribution Function) of the PL. Figures A6, A7, and A8 are plots of the PL CDF for the urban, suburban, and rural zones, respectively.

FIGURE A6
PL CDF for Urban Cells

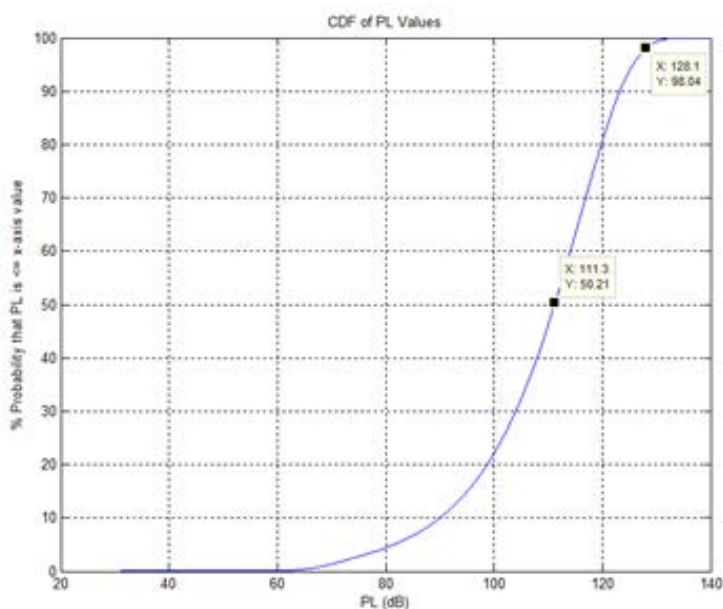


FIGURE A7
PL CDF for Suburban Cells

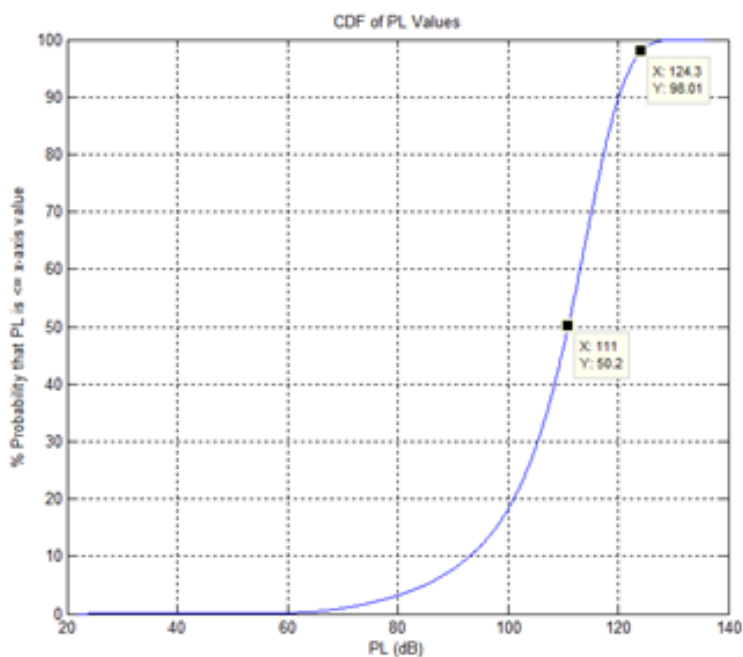
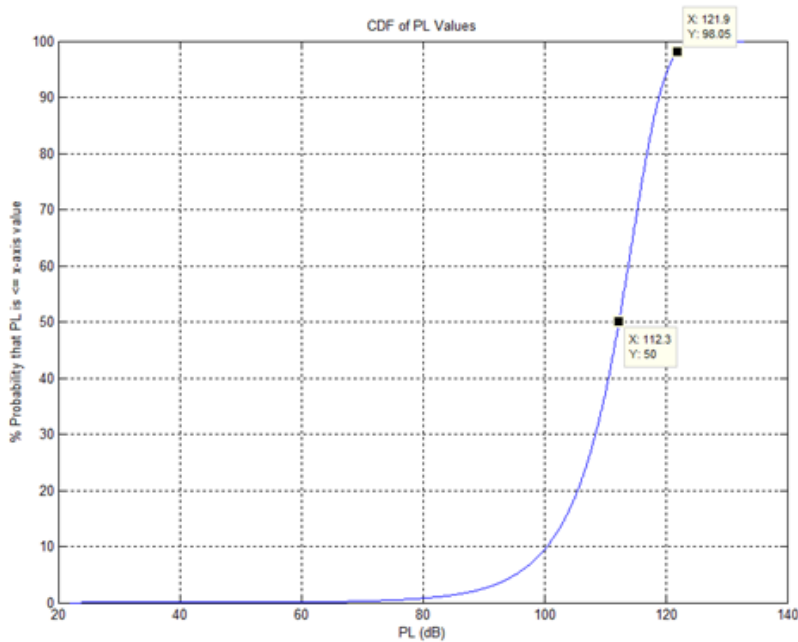


FIGURE A8
PL CDF for Rural Cells



Step 10

From the CDFs, select a PL percentile value based on the % of UEs assumed to operate at max transmit power. Section 2.3 of the Annex 2 document discusses proper assumptions for UE uplink power control (UPC) and notes that LTE UPC has both open loop and closed loop components, but that for Monte-Carlo simulations, the open loop model is mainly used. This model sets the UE transmit power based on the PL between the UE and its serving base-station along with other parameters, including one which corresponds to the % of active users transmitting at maximum power (P_{max}). The Annex 2 document suggests that the % of UEs in macro-cells transmitting at P_{max} be in the 2%-5% range. This analysis assumes 2%. Therefore, according to the UE UPC formula in Step 2 of section 2.2.2 of the Annex 2 document, UEs whose PL exceed the 98%-percentile PL value will transmit at P_{max} . Conversely, UEs whose PL \leq the 98%-percentile PL value will transmit at a power level less than P_{max} . The 98% PL values for the urban/suburban/rural cells are indicated in Figures A6, A7, and A8.

These values are $PL_{x-ile} = 128.1$ dB (urban); 124.3 dB (suburban); 121.9 dB (rural)

Thus, for example for the rural cells, the CDF in Figure A8 indicates that 98% of the UEs have PL less than or equal to 121.9 dB while 2% of the UEs have PL exceeding 121.9 dB. Therefore, that 2% of UEs is assumed to transmit at maximum power (e.g $P_{max} = +23$ dBm/200 mW).

Step 11

Specify other UE uplink power control parameters used in the Annex 2 UPC formula.

In this analysis we assume $P_{max} = +23$ dBm; $P_{min} = -40$ dBm (min UE tx power); $\gamma = 1$ (gamma is a value between 0 and 1 called the balancing factor); and $R_{min} = P_{min}/P_{max}$.

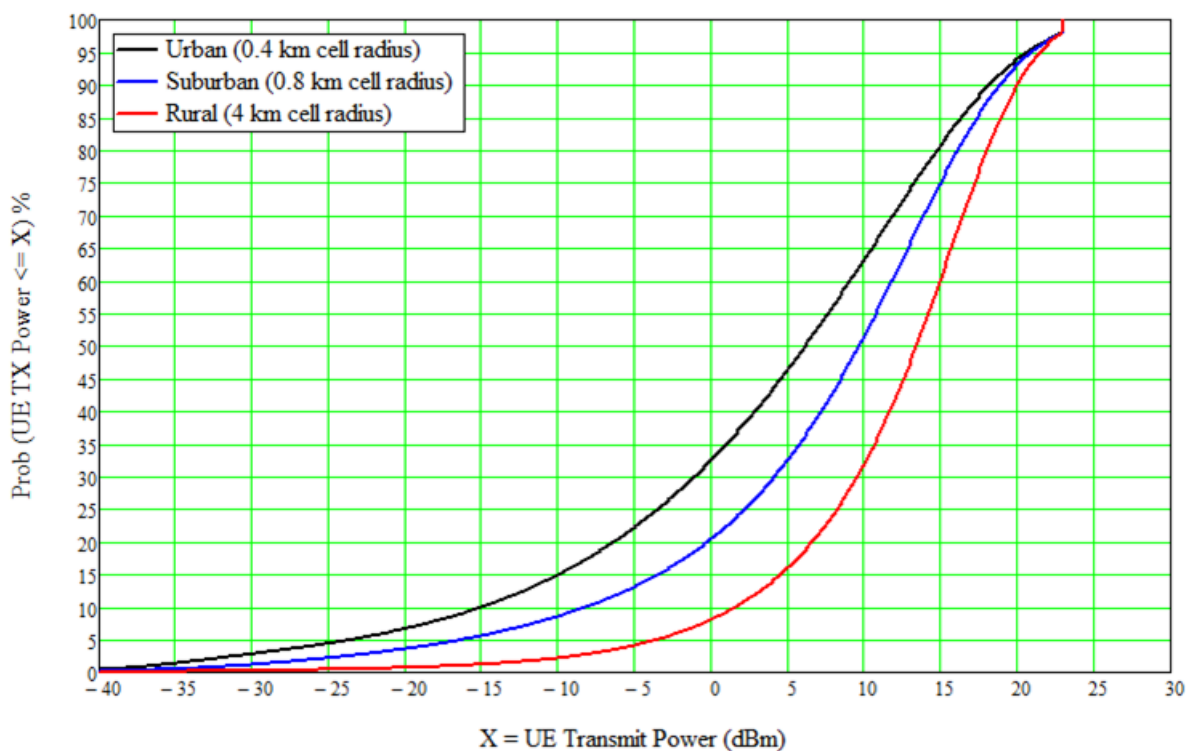
Step 12

Now apply the UPC formula to the PL values from Step 8 to get the corresponding UE transmit power values and from these we can generate the UE transmit power CDFs. From section 2.2.2 of the Annex 2 document, the UPC formula for the UE transmit power (P_t) (in dBm) in terms of the above parameters is given by:

$$P_t = P_{\max} \times \min \left\{ 1, \max \left[R_{\min}, \left(\frac{PL}{PL_{x-ile}} \right)^\gamma \right] \right\}$$

The resulting (single) UE transmit power CDFs are shown in Figure A9.

FIGURE A9
UE transmit power CDFs for urban/suburban/rural zones



Step 13

From the LTE cell layout pattern in Figure A1 determine the number of simultaneously transmitting UEs in the urban/suburban/rural zones.

Referring to Figure A1, there are 89 base-station sites/267 cells in the urban zone. Assuming 6 active UEs per cell (per Annex 2 doc), this results in a total of $267 \times 6 = 1\,602$ UEs. However, it is assumed in the analysis that 70% of these UEs are indoors and not contributing any interference. Therefore, only 30% of these UEs are assumed to be interfering UEs so that $N_{UE} = 0.3 \times 1\,602 = 480$.

For the suburban zone there are 996 base-station sites/2988 cells so that total number of UEs is $6 \times 2\,988 = 17\,928$. Again, however, 70% of these are assumed to be indoors contributing no interference.

So in this case the number of interfering UEs is $N_{UE} = 0.3 \times 17\,928 = 5\,378$.

For rural zone there are 216 base-station sites/648 cells so that total number of UEs is $6 \times 648 = 3\,888$. However, 50% of these are assumed to be indoors contributing no interference. So in this case the number of interfering UEs is $N_{UE} = 0.5 \times 3\,888 = 1\,944$.

Step 14. Using the urban/suburban/rural (single) UE transmit power CDFs from Step 12 and the number of simultaneously interfering UEs per zone from Step 13, perform another set of Monte Carlo trials to get the distribution and mean values of the *aggregate* UE power per zone.

This involves performing a large number of trials (N trials) for each zone and for the nth trial:

- a) generate N_{UE} random samples of UE transmit power using the appropriate CDF from Step 12 (e.g. for urban zone, generate 480 samples of random UE transmit power using the urban CDF in Figure A9);
- b) convert the sample UE transmit power values from dBm to mW; sum them to get the aggregate power (in mW); then convert back to dBm to get the aggregate power in dBm;
- c) repeat steps a and b a large number of times (e.g. $N = 100,000$ trials) to get N sample values of the aggregate power (i.e. a vector V containing N sample values of aggregate power);
- d) determine the aggregate power statistics using the above agg power vector (V).

This results in the following statistics for the 3 zones:

	URBAN	SUBURBAN	RURAL
min agg power value (dBm):	$\min(V) = 38.584294$	$\min(V) = 51.148747$	$\min(V) = 48.282791$
max agg power value (dBm):	$\max(V) = 41.076193$	$\max(V) = 51.815593$	$\max(V) = 49.113556$
mean agg power value (dBm):	$\text{mean}(V) = 39.964658$	$\text{mean}(V) = 51.479832$	$\text{mean}(V) = 48.705754$
standard deviation of agg power samples (dBm):	$\text{stdev}(V) = 0.337691$	$\text{stdev}(V) = 0.084058$	$\text{stdev}(V) = 0.109614$

Note that the aggregate power distribution is very narrow (looking at standard deviation values and min/max values). This is due to the “law of large numbers” effect. Even though the power distribution of a single UE can have a large variance (i.e. -40 to $+23$ dBm), the aggregate power distribution of a large number of UEs has a relatively small variance. So in the simulations, we assume the mean aggregate power values above as the effective UE power per zone values.

APPENDIX B

Aggregate LTE base-station power for cities

Method for calculating aggregate LTE base-station power for worldwide cities

This Appendix describes the methodology used to compute aggregate LTE base-station (BS) power for the urban/suburban/rural zones used in the simulations. For each city, 3 “effective” base-stations are modelled in the simulation – representing the 3 city zones (urban/suburban/rural) – and are assumed to be co-located at the city centre. It is necessary to model 3 effective BSs per city since the BSs in each zone have different sector antenna gains and downtilt angles. Specifically, urban BSs are assumed to have a sector antenna gain of 16 dBi with a 10° downtilt; suburban BSs are assumed to have a sector antenna gain of 16 dBi with a 6° downtilt; and rural BSs are assumed to have a sector antenna gain of 18 dBi with a 3° downtilt.

Therefore, for each zone, it is necessary to determine the net effective power of the effective base-station representing that zone. As in the case of the UEs, simulations have been performed that demonstrate that using this effective base-station approach yields essentially the same interference results into the satellite receiver as modelling each individual base-station site in the LTE deployment pattern. Thus, using this effective base-station approach is a valid assumption for the purpose of calculating aggregate interference into satellite receivers while having the advantage of significantly reducing simulation time.

To determine the net power for the effective BS, we again refer to the LTE deployment pattern shown in Figure A1 and perform the following steps for each zone.

Step 1

Determine the number of interfering base-station sites per zone.

Referring to Figure A1, there are 89 base-station sites in the urban zone. However, it is assumed in the analysis that 50% of the base-station site antennas (20 metres height) are below the urban rooftop level and we make the conservative assumption that *none* of the base-station sites below rooftop level contribute to the interference. Therefore, for the urban zone, we assume the number of interfering base-station sites is $N_{BS} = 0.5 \times 89 = 44$ base-station sites.

There are 996 base-station sites in the suburban zone and the antennas of all these sites (25 metres height) are assumed to be above suburban rooftop level, so the number of interfering base-station sites in this case is $N_{BS} = 996$ base-station sites.

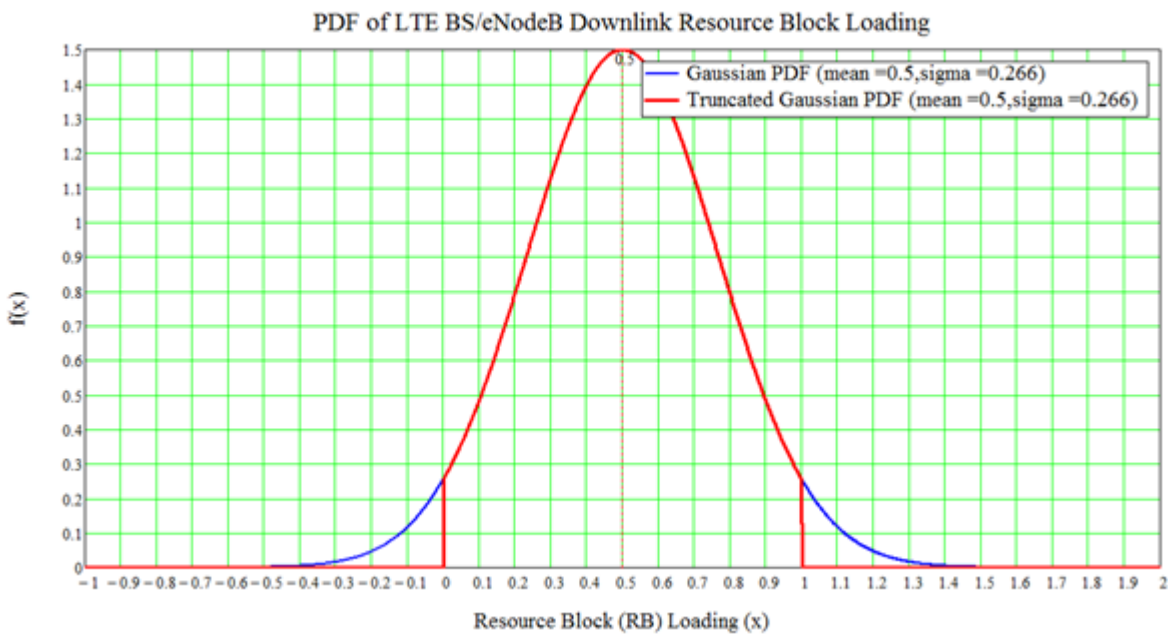
There are 216 base-station sites in the rural zone and the antennas of all these sites (30 metres height) are assumed to be above rooftop level, so the number of interfering base-station sites for rural case is $N_{BS} = 216$ base-station sites.

Step 2

Define the probability distribution function (PDF) for base-station (eNB) transmit power. It is recognized that LTE base-stations do not operate at maximum power all the time. In the analysis, it is assumed that base-station transmit power is proportional to resource block (RB) loading on the downlink (i.e. if only half of the RBs are active, then the base-station is only operating at half max power). The PDF for the RB loading is shown in Figure B1 and is a truncated Gaussian PDF with a mean value of 50% corresponding to base-station transmit power equal to 50% of maximum power. In the simulation, a 10 MHz LTE channel bandwidth (50 RBs) with a maximum transmit power of $P_{max} = 46$ dBm (40W) is assumed. (Note: this is the power output from the eNB transmitter prior to 3 dB feeder/line loss and prior to the sector antenna input.)

The PDF is truncated to ensure the RB loading is always between 0 (no loading with 0W transmit power) and 1 (100% loading with transmit power = max power = 40W). Further, the standard deviation of the PDF is chosen equal to 0.266 corresponding to a call blocking probability of 3% (i.e. the area under the Gaussian curve above $x = 1$ is 0.03 implying that there is a 3% chance that a new UE cannot connect to the network because all RBs are already active and base-station is at maximum transmit power).

FIGURE B1
Assumed Probability Distribution of base-station Resource Block Loading/TX Power



Step 3

Using the PDF in Step 2 and the number of interfering base-station (N_{BS}) in Step 1, perform a large number of Monte-Carlo trials (N) to determine the aggregate power for the effective base-station for each zone. Therefore, for the n th trial, perform the following steps:

- a) generate N_{BS} random samples of RB loading (α) according to the above truncated Gaussian PDF;
- b) compute the corresponding values of transmit power (in watts) based on the RB loading values (α) and the max power ($p_{max} = 40W$) (i.e. $p_t = \alpha p_{max}$);
- c) sum up all the transmit power values in step b (sum in watts); then convert to dBm to get the aggregate transmit power value for the n th trial;
- d) repeat steps a-c for N trials to get an N -element vector (V) of aggregate power values (in dBm).

Step 4

Compute statistics of the aggregate power distribution from vector V. The results of doing this Monte-Carlo procedure for the 3 zones are shown below.

	URBAN	SUBURBAN	RURAL
Min value of agg power (dBm)	min(V) = 58.109442	min(V) = 72.73358	min(V) = 65.783809
Max value of agg power (dBm)	max(V) = 60.569696	max(V) = 73.216261	max(V) = 66.830232
Mean agg power (dBm)	mean(V) = 59.433596	mean(V) = 72.994869	mean(V) = 66.350378
Standard deviation of agg power samples (dBm)	stdev(V) = 0.331094	stdev(V) = 0.069576	stdev(V) = 0.150746

Note again that the aggregate power distribution is very narrow (looking at standard deviation values and min/max values). This is due to the “law of large numbers” effect. Even though the power distribution of a single base-station can have a large variance, the aggregate power distribution of a large number of BSs has a relatively small variance. So in the simulations, we assume the mean aggregate power values above as the effective base-station power per zone values.

Also, note that because the mean loading is assumed to be 50%, the aggregate mean values above can be very nearly reproduced using just the mean base-station power (i.e. 20 W) and the number of interfering base-station (N_{BS}):

For urban: $10\log(20 \times 44) + 30 = 59.44$ dBm

For suburban: $10\log(20 \times 996) + 30 = 72.99$ dBm

For rural: $10\log(20 \times 216) + 30 = 66.35$ dBm

For the 20% base-station loading case (mean base-station power = $0.2 \times 40W = 8W$), the aggregate values are:

For urban: $10\log(8 \times 44) + 30 = 55.46$ dBm

For suburban: $10\log(8 \times 996) + 30 = 69.01$ dBm

For rural: $10\log(8 \times 216) + 30 = 62.37$ dBm

These power levels are then applied to the input of the sector antenna in Appendix C (after subtracting 3 dB feeder/line loss) and using the appropriate gain and downtilt for the particular zone.

APPENDIX C

LTE base-station sector antenna pattern

The LTE base-station sector antenna pattern is based on the sector antenna pattern in Recommendation ITU-R F.1336. The average sidelobe pattern in *recommends* 3.1.2 of Recommendation ITU-R F.1336 is assumed.

The G_{hr} and G_{vr} equations are exactly the same as shown in Recommendation ITU-R F.1336:

- the normalized elevation angle $x_v = \theta/\theta_3$
- the relative vertical pattern $G_{vr}(x_v)$ is multiplied by a compression ratio, R , which weights the vertical gain as the azimuth angle varies from 0 to φ . Therefore, the composite relative gain pattern is given by:

$$G_R(\varphi, \theta) = G_{hr}\left(x_h = \frac{\varphi}{\varphi_3}\right) + R(\varphi) \cdot G_{vr}\left(x_v = \frac{\theta}{\theta_3}\right)$$

where the compression factor R is defined as:

$$R(\varphi) = \frac{G_{hr}\left(x_h = \frac{\varphi}{\varphi_3}\right) - G_{hr}\left(x_h = \frac{180}{\varphi_3}\right)}{G_{hr}(x_h = 0) - G_{hr}\left(x_h = \frac{180}{\varphi_3}\right)}$$

In these equations the azimuth angle φ varies from -180 to 180 degrees and the elevation angle θ varies from -90 to 90 degrees. The main beam gain is in the direction of ($\varphi=0, \theta=0$); the principal EL plane is defined by ($\varphi=0, \theta = -90$ to 90); and the principal AZ plane is defined by ($\varphi = -180$ to $180, \theta = 0$).

Sample plots of this sector antenna pattern are shown below assuming the following additional parameters that define the pattern:

Main beam gain = $G_o = 16$ dBi

Azimuth plane HPBW (full-angle) = $\varphi_3 = 65$ degrees

Elevation plane HPBW (full-angle) = $\theta_3 = 11.98$ degrees

Note: θ_3 is calculated as a function of G_o and φ_3 using equation (3) of section 3.3 of Recommendation ITU-R F.1336 which is: $\theta_3 = 31000 \times 10^{(-0.1G_o)/\varphi_3}$

k-parameters: $k_a = 0.7$; $k_h = 0.7$; $k_v = 0.3$

The principal EL plane pattern in both rectangular and polar coordinates is shown in Figures C1 and C2.

FIGURE C1

Principal EL Plane Pattern in Rectangular Coordinates

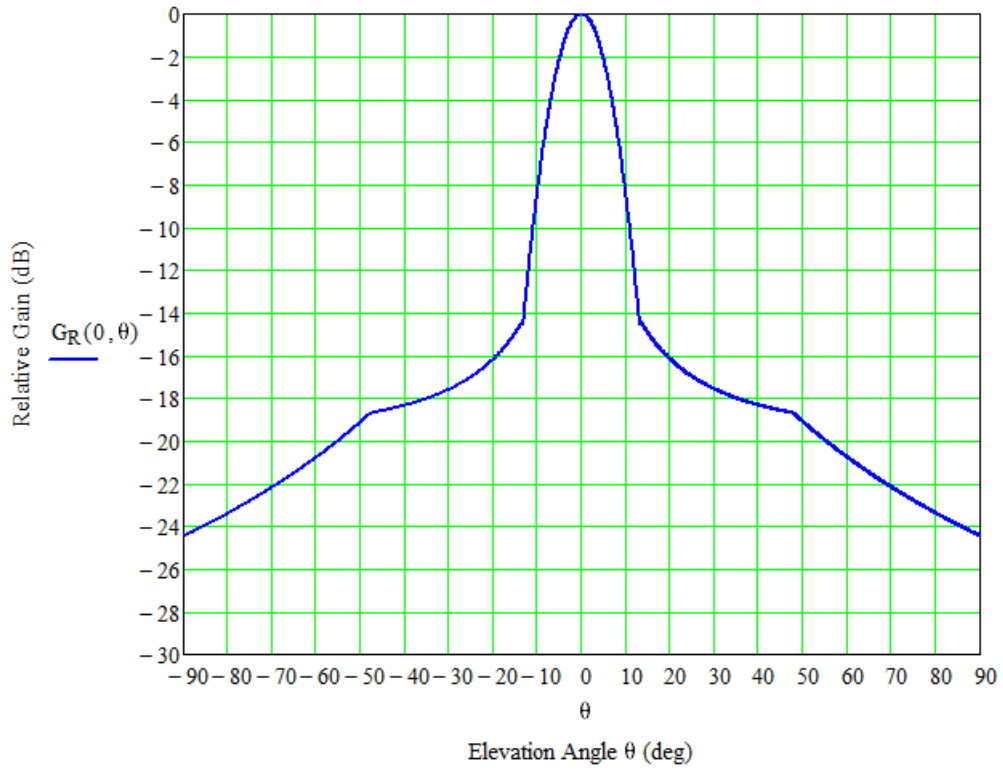
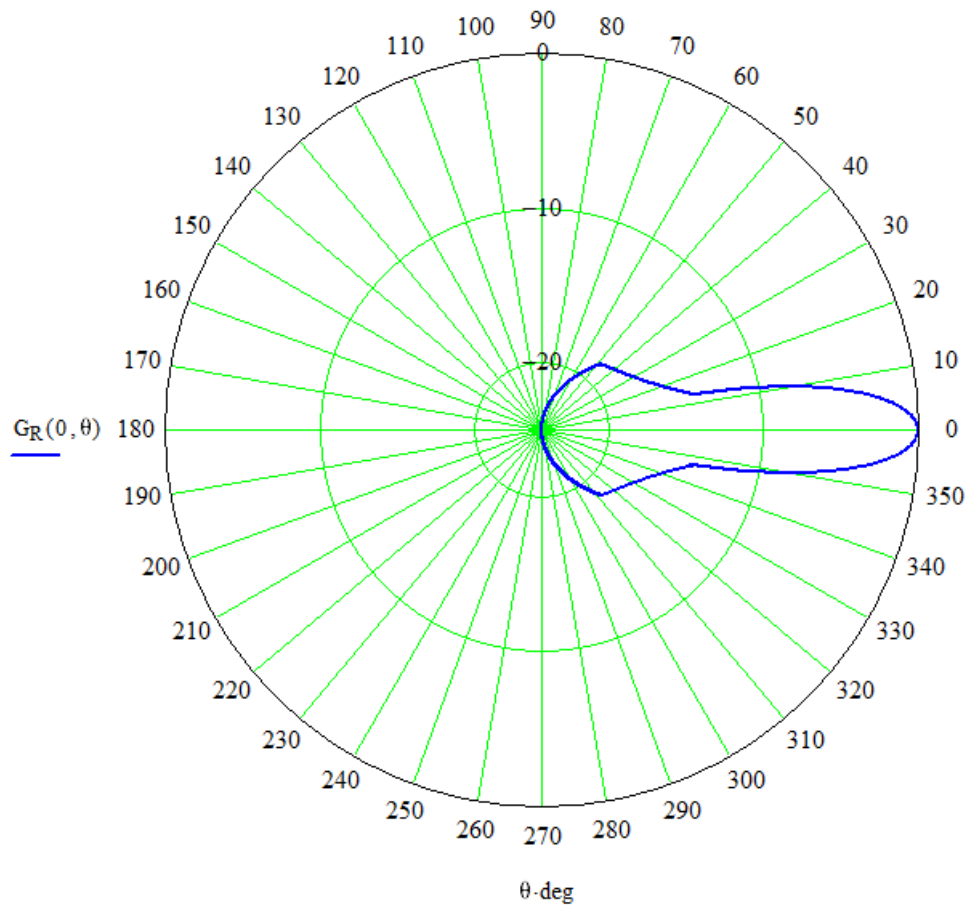


FIGURE C2
Principal EL Plane Pattern in Polar Coordinates



The principal AZ plane pattern in both rectangular and polar coordinates is shown in Figures C3 and C4.

FIGURE C3
Principal AZ Plane Pattern in Rectangular Coordinates

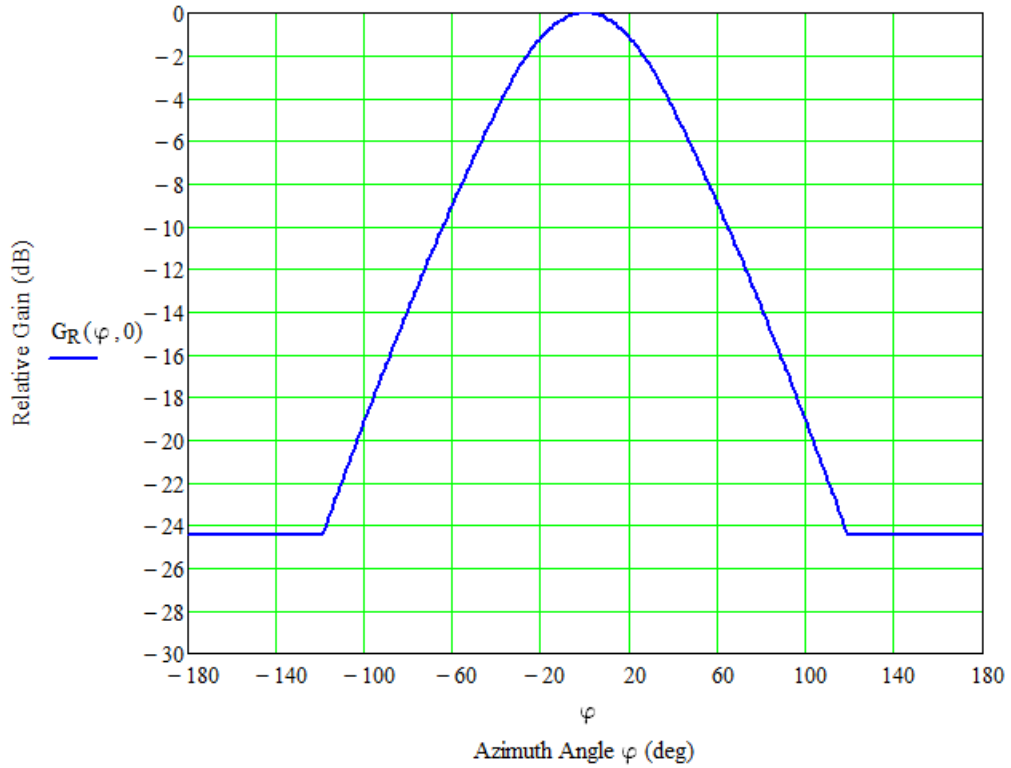
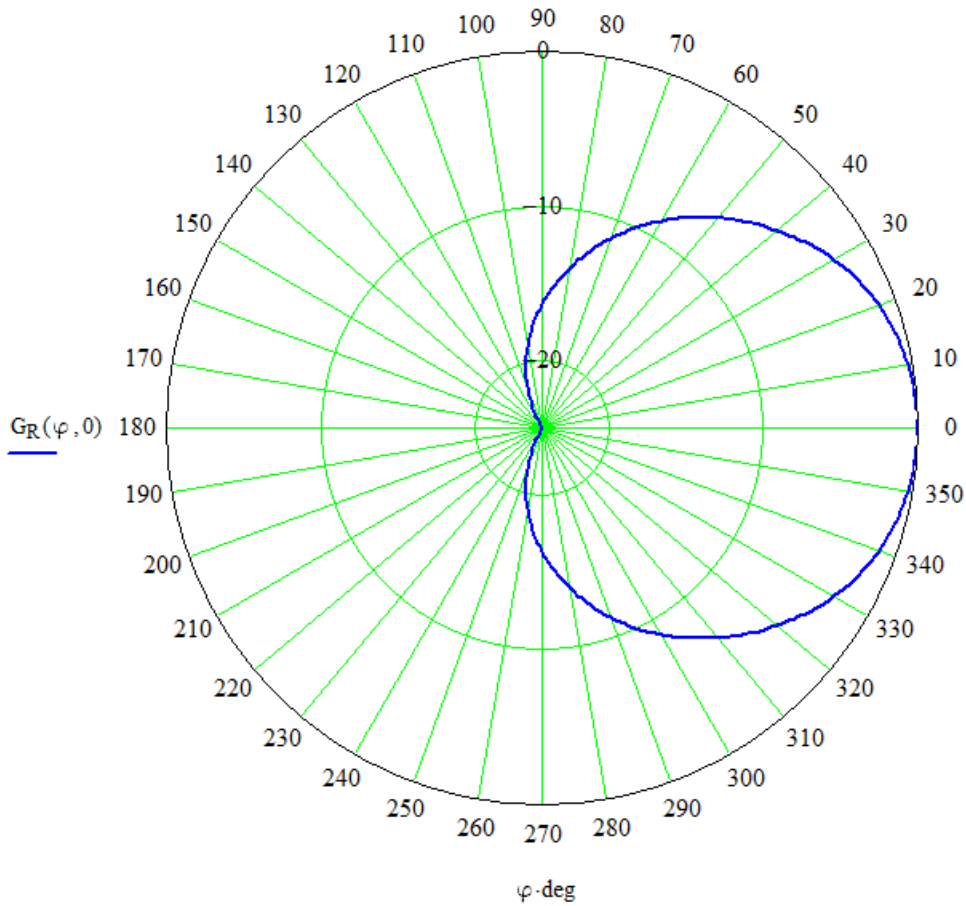


FIGURE C4
Principal AZ Plane Pattern in Polar Coordinates



Figures C5-C7 show the 3D pattern from oblique, top-down, and side views. It should be noted that in these 3D plots, the actual minimum gain value of the pattern is $G_{180} = -24.5$ dB and the maximum gain value is 0 dB. But in order to plot the pattern as a 3D surface the gains must be treated as non-negative radii. Therefore a constant gain adjustment factor of $K = |G_{180}| = +24.5$ dB is added to all the gain values (i.e. the min gain value of -24.5 dB is assumed to have 0 radius). Therefore the actual relative gain value from the 3D pattern is the radius measured from the origin minus K .

FIGURE C5
Oblique View of 3D Pattern

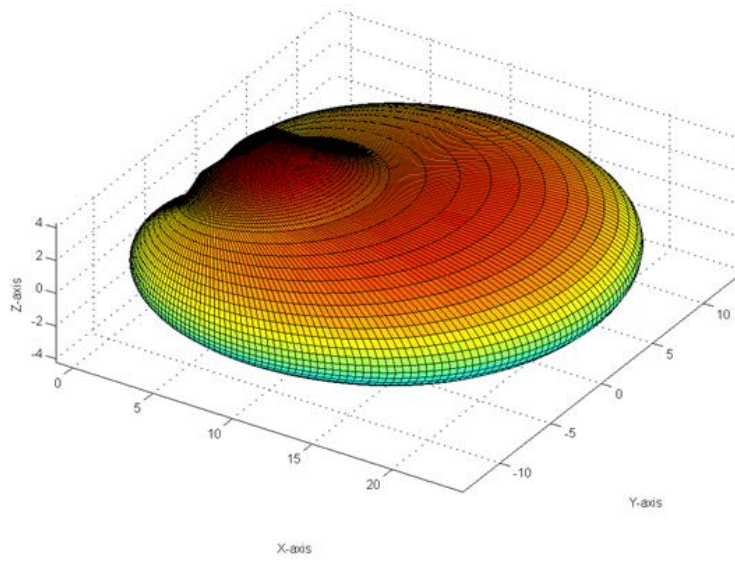


FIGURE C6
Top Down View of 3D Pattern

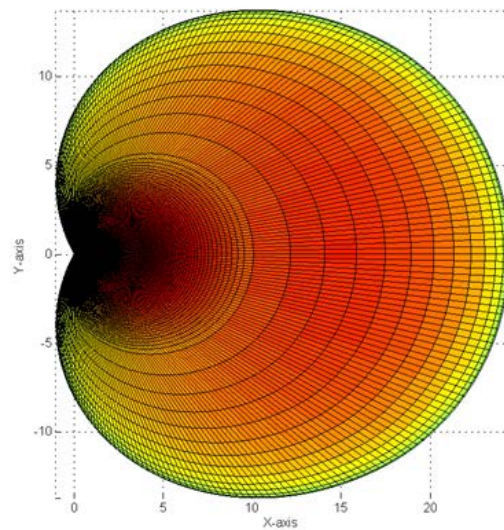
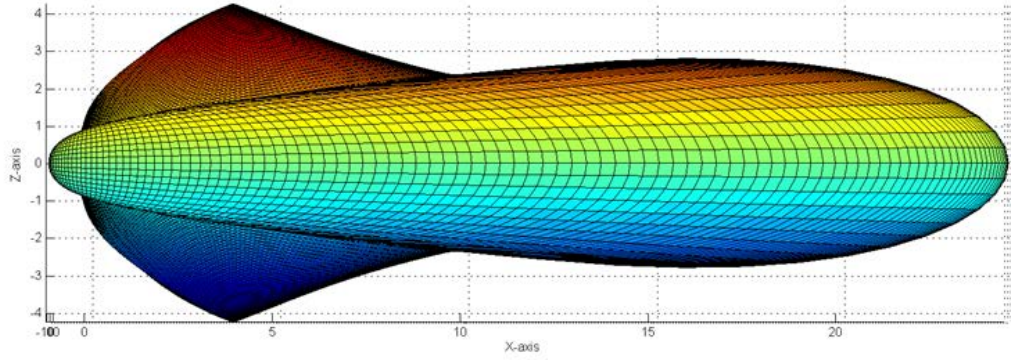


FIGURE C7
Side View of 3D Pattern



APPENDIX D

Method for applying Recommendation ITU-R P.452 clutter model

This Appendix describes the methodology used to apply the clutter model of Recommendation ITU-R P.452 § 4.5.3. The model, which is intended to be used for interference from one point on the Earth to another point on the Earth, has a clutter model which is applied by:

- 1 calculate the clutter losses at either one or both ends of the link using a set of clutter categories and nominal values of clutter height and distance;
- 2 assume the transmitter or receiver or both, which is imbedded in the clutter, is moved to the opposite side of the clutter. (i.e., Place the antenna(s) imbedded in clutter at the nominal clutter height);
- 3 calculate the rest of the losses as though there was no clutter using the new antenna placement(s) and add the clutter losses from step 1 at the end.

Since the application of Recommendation ITU-R P.452, as a terrestrial point-to-point model, assumes the propagation paths will be relatively horizontal than most cases as compared to signals going up to an aircraft or spacecraft (as considered in this analysis). This would generally make the propagation path through the clutter longer and, consequentially, clutter losses greater. Thus, this clutter model can be used as a worst case (i.e. maximum attenuation) for a scenario of a transmitter imbedded in clutter and receiver on a spacecraft. The application of this model as used in this analysis is described below:

- **Step 1:** Apply clutter categories, heights and distances as provided in Table 4 of Recommendation ITU-R P.452. The representative clutter categories as applied to the Recommendation ITU-R P.452 clutter categories with the rural, suburban, and urban categories used in the analysis is presented in Table D1, below.

TABLE D1
Listing of Recommendation ITU-R P.452 clutter categories

Nominal clutter heights and distances			
Clutter (ground-cover) category		Nominal height, h_a	Nominal distance, d_k
		(m)	(km)
Rural	High crop fields	4	0.1
	Park land		
	Irregularly spaced sparse trees		
	Orchard (regularly spaced)		
	Sparse houses		
Suburban	Suburban	9	0.025
	Dense suburban	12	0.02
Urban	Urban	20	0.02
	Dense urban	25	0.02
	High-rise urban	35	0.02

- **Step 2:** Calculate clutter attenuation using equations (47) and (47a) of Recommendation ITU-R P.452.
- **Step 3:** Use equation $\text{atan}((h-h_a)/d_k)$ to calculate the maximum elevation angle for the interfering clutter path for each city and apply the appropriate clutter loss for that city, where h is the height of the UE terminal, h_a is the nominal clutter height, and d_k is the nominal distance.

The attached Excel spreadsheet presents a sample calculation utilizing the methods described above. This sample calculation assumes a macro cell in an urban area, where the height of the LTE station (L10) is 20 meters. The nominal clutter height (D27) is 35 meters and the horizontal clutter distance (E27) is 20 meters. Using equations (47) and (47a) of Recommendation ITU-R P.452, the clutter loss (L27) is 12.8 dB and the angle from the transmitter to the top of the clutter height (M27) is $\text{atan}((35-20)/20)=36.9$ degrees. Therefore, if the aircraft/spacecraft is at an elevation angle at or below 36.9 degrees, 12.8 dB of clutter loss should be added. If the spacecraft is above 36.9 degrees, there is no clutter loss.



UEClutterCalc.xlsx

APPENDIX E

List of Worldwide cities used in analyses

TABLE E1

List of 160 Major Cities Used in LTE-TDRSS Interference Simulations

CITY #	CITY	LAT	LON	POP	EL to 41W TDRS	AZ to 41W TDRS
1	Adana	37.06	35.39	1849473	2.14	-98.27
2	Albuquerque	35.11	-106.61	448607	11.22	104.59
3	Alexandria	31.30	30.41	4150000	7.18	-99.89
4	Algiers	36.79	3.04	3390000	27.45	-121.74
5	Amman	31.74	35.92	2530000	2.41	-96.94
6	Amsterdam	52.37	4.89	743079	16.85	-127.49
7	Ankara	39.78	32.95	3810000	3.60	-100.40
8	Arequipa	-16.39	-71.44	783000	50.26	64.38
9	Arlington CDP	38.88	-77.11	332969	31.59	130.69
10	Asuncion	-25.12	-57.51	513399	55.32	34.96
11	Athens	38.02	23.52	3730000	11.29	-106.33
12	Atlanta	33.77	-84.35	4160000	29.66	120.46
13	Austin	30.30	-97.75	656562	20.10	108.28
14	Bahia Blanca	-38.73	-62.26	301572	40.01	31.90
15	Baltimore	39.31	-76.62	651154	31.59	131.46
16	Bamako	12.66	-8.03	1016296	49.28	-108.64
17	Barcelona	41.40	2.16	4040000	25.33	-125.16
18	Beirut	34.04	35.64	1303129	2.36	-97.55
19	Belem	-1.24	-48.32	1407737	81.26	80.42
20	Belgrade	44.80	20.50	1306168	11.27	-110.90
21	Belo Horizonte	-19.89	-43.95	4640000	66.46	8.63
22	Berlin	52.43	13.08	3690000	12.49	-119.84
23	Birmingham	52.50	-2.26	2310000	20.21	-134.66
24	Bogota	4.59	-74.08	7440000	51.20	97.00
25	Bordeaux	44.85	-0.62	1105000	24.82	-129.64
26	Boston	42.41	-71.13	4750000	32.37	139.26
27	Brasilia	-15.72	-47.76	2383784	69.96	23.65
28	Bucharest	44.44	26.11	2000000	7.51	-106.44
29	Budapest	47.50	19.13	1697117	11.14	-112.92
30	Buenos Aires	-34.60	-58.48	12390000	45.69	29.04
31	Buffalo	42.68	-78.91	1135509	27.79	131.01
32	Cairo	30.09	31.29	16750000	6.63	-99.07
33	Cali	3.72	-75.24	2500000	50.00	95.44
34	Cape Town	-33.96	18.48	2900000	16.58	-71.80
35	Caracas	10.47	-66.62	2670000	57.84	110.73
36	Casablanca	33.60	-7.62	2930000	37.16	-130.00
37	Charlotte	35.21	-80.83	540828	31.47	124.63
38	Chicago	41.97	-87.80	9030000	22.58	122.10
39	Cincinnati	39.15	-84.46	2896016	26.49	123.64
40	Cleveland	41.50	-81.61	478403	26.92	127.67

CITY #	CITY	LAT	LON	POP	EL to 41W TDRS	AZ to 41W TDRS
41	Colorado Springs	38.86	-104.79	360890	11.60	107.14
42	Columbus	39.99	-82.99	711470	26.98	125.50
43	Conakry	9.56	-13.56	1091500	56.24	-107.72
44	Copenhagen	55.71	12.46	1167569	11.09	-121.45
45	Cordoba	-31.31	-64.34	1428214	45.61	39.73
46	Corpus Christi	27.74	-97.40	277454	21.23	107.16
47	Cracov	50.10	20.07	755050	9.52	-112.95
48	Curitiba	-25.45	-49.26	2900000	58.87	18.69
49	Dakar	14.75	-17.38	2650000	57.76	-120.17
50	Dallas	32.78	-96.80	5160000	20.05	110.17
51	Damaskus	33.64	36.70	2240000	1.53	-96.86
52	Denver	39.69	-104.94	2180000	11.24	107.31
53	Detroit	42.46	-83.05	3860000	25.38	126.78
54	Dublin	53.30	-6.23	495781	21.33	-139.09
55	Durban	-29.85	30.96	3070000	6.95	-80.82
56	Edinburgh	55.89	-2.84	448624	17.91	-136.47
57	Edmonton	53.55	-113.52	817498	1.60	104.19
58	El Paso	31.79	-106.42	563662	12.21	103.52
59	Fortaleza	-3.58	-38.96	3160000	85.15	-29.75
60	Frankfurt	50.11	8.67	2320000	16.19	-123.05
61	Fresno	36.78	-119.79	427652	0.27	96.74
62	Gdansk	54.25	18.69	461865	8.57	-115.36
63	Glasgow	55.88	-4.25	577670	18.49	-137.93
64	Guadalajara	20.68	-103.36	4090000	17.43	100.46
65	Guatemala	14.63	-90.55	1022001	31.47	102.13
66	Guayaquil	-2.20	-79.90	2530000	44.89	87.28
67	Hamburg	53.57	10.08	1704735	13.47	-122.98
68	Harare	-17.98	30.86	1435784	8.62	-84.24
69	Havana	23.09	-82.38	2190000	36.69	113.97
70	Helsinki	60.06	23.98	562713	3.53	-111.99
71	Houston	29.71	-95.39	4550000	22.35	109.52
72	Indianapolis	39.79	-86.15	781870	24.95	122.46
73	Istanbul	41.07	29.00	11220000	6.31	-103.42
74	Izmir	38.42	27.11	2480000	8.39	-103.99
75	Jacksonville	30.32	-81.66	735617	33.69	120.42
76	Jerusalem	31.72	34.97	726638	3.22	-97.46
77	Johannesburg	-26.15	28.05	6470000	10.16	-80.45
78	Khartoum	15.62	32.54	700887	7.21	-94.53
79	Kingston	18.00	-76.81	579137	44.26	113.16
80	La Paz	-16.49	-67.90	835167	53.63	60.79

CITY #	CITY	LAT	LON	POP	EL to 41W TDRS	AZ to 41W TDRS
81	Las Vegas	36.19	-115.22	478434	4.01	99.44
82	Lexington-Fayette	38.03	-84.49	260512	27.13	122.97
83	Lisbon	38.77	-9.37	2340000	34.45	-135.44
84	London	51.52	-0.13	8320000	19.92	-132.11
85	Los Angeles	34.00	-118.20	14730000	1.89	97.21
86	Louisville	38.23	-85.75	3694820	26.12	121.95
87	Madrid	40.43	-3.68	5130000	29.72	-130.36
88	Manaus	-3.06	-60.07	1688524	67.36	81.22
89	Maracaibo	10.65	-71.64	1706547	52.45	107.31
90	Marseille	43.47	5.17	796525	22.14	-123.41
91	Medellin	6.44	-75.75	3080000	49.05	99.17
92	Memphis	35.11	-90.04	672277	24.54	116.51
93	Mexico City	19.41	-99.10	8851080	21.83	101.67
94	Miami	25.83	-80.24	5220000	37.29	118.05
95	Milan	45.47	9.18	4190000	18.45	-120.70
96	Milwaukee	43.06	-87.97	578887	21.85	122.48
97	Minneapolis	44.90	-93.36	2570000	17.35	118.54
98	Minsk	53.88	27.59	1789098	3.76	-107.55
99	Monterrey	25.81	-100.51	3650000	18.96	104.36
100	Montevideo	-34.89	-56.12	1345010	46.39	25.30
101	Montreal	45.52	-73.61	3360000	28.56	138.09
102	Munich	48.19	11.23	1326807	15.75	-119.98
103	Naples	40.85	14.26	3010000	17.24	-114.37
104	Nashville-Davidson (balance)	36.15	-86.76	545524	26.52	119.85
105	New Orleans	29.96	-90.12	343829	26.80	113.35
106	New York	40.70	-73.93	20090000	32.19	135.17
107	Nouakchott	17.91	-15.96	558195	54.52	-123.33
108	Odessa	46.52	30.61	989468	3.87	-103.53
109	Oklahoma City	35.48	-97.53	506132	18.44	110.96
110	Omaha	41.26	-96.01	390007	17.24	114.75
111	Oslo	59.95	10.75	586860	9.50	-124.28
112	Ottawa	45.32	-76.19	812135	27.38	135.22
113	Palermo	38.05	13.41	668686	19.07	-113.77
114	Paris	48.87	2.41	10430000	20.41	-128.50
115	Philadelphia	40.01	-75.12	5270000	32.01	133.47
116	Phoenix	33.46	-112.07	3540000	7.08	100.68
117	Pittsburgh	40.47	-79.87	1753136	28.72	128.82
118	Porto Alegre	-30.10	-51.27	3440000	53.17	19.88
119	Prague	50.08	14.42	1176116	12.90	-117.84
120	Quebec	46.65	-71.23	7903000	28.78	141.26

CITY #	CITY	LAT	LON	POP	EL to 41W TDRS	AZ to 41W TDRS
121	Quito	-0.17	-78.49	1482447	46.54	89.77
122	Rabat	33.96	-6.77	673000	36.31	-129.35
123	Raleigh	35.82	-78.64	276093	32.65	127.16
124	Recife	-8.09	-34.92	3490000	78.11	-37.14
125	Rio de Janeiro	-22.88	-43.39	11160000	63.09	6.13
126	Riverside	33.95	-117.40	255166	2.57	97.67
127	Rome	41.93	12.50	2761477	18.02	-116.28
128	Rosario	-32.89	-60.83	907718	46.19	33.61
129	Salt Lake City	40.68	-111.84	1145905	5.77	102.73
130	Salvador	-12.66	-38.44	2980000	74.83	-11.55
131	San Antonio	29.46	-98.52	1256509	19.70	107.35
132	San Diego	32.78	-117.04	2790000	3.02	97.64
133	San Jose	9.89	-84.03	912332	39.35	100.41
134	San Juan	18.44	-66.12	2380000	54.12	123.97
135	San Juan zona urbana	18.41	-66.06	421958	54.19	124.01
136	Santa Ana	33.74	-117.88	337977	2.19	97.35
137	Santa Fe	-31.69	-60.80	1397692	47.32	34.45
138	Santiago	-33.37	-70.83	836614	39.77	46.22
139	Santo Domingo	18.51	-69.84	673234	50.67	119.93
140	Sao Paulo	-23.57	-46.68	19140000	61.70	13.97
141	Sevilla	37.20	-5.94	704414	33.46	-130.71
142	Sofia	42.84	23.62	1151220	9.75	-107.85
143	St. Louis	38.67	-90.32	2160000	22.58	118.21
144	St. Paul	44.95	-93.11	287151	17.48	118.77
145	Stockholm	59.30	18.03	776962	6.61	-117.27
146	Tampa	27.97	-82.46	303447	34.27	117.93
147	Tegucigalpa	14.30	-87.32	858437	34.89	103.26
148	Toledo	41.67	-83.58	313619	25.55	125.86
149	Toronto	43.70	-79.44	5790000	26.75	131.01
150	Tripoli	32.79	13.31	1500000	21.28	-111.23
151	Tucson	32.21	-110.92	486699	8.29	101.00
152	Tulsa	36.13	-95.94	393049	19.46	112.45
153	Tunis	36.80	10.17	2270000	22.09	-115.71
154	Vienna	48.20	16.34	1651437	12.61	-115.51
155	Vilnius	55.15	25.82	542303	4.34	-109.34
156	Virginia Beach	36.83	-76.09	425257	33.70	130.45
157	Warsaw	52.24	20.99	2020000	8.12	-112.78
158	Washington D.C.	38.89	-77.03	4260000	31.63	130.77
159	Wichita	37.69	-97.34	344284	17.75	112.13
160	Zagreb	45.52	15.85	691724	14.11	-114.95